Enhancement of Flow properties and Flowability of Pharmaceutical Excipients (MCCP) and its Effect on Tabletability

A Dissertation Submitted

in partial fulfilment of requirements
for the degree of

Master of Engineering

in

Thermal Engineering

by

Krishang Kashyap

Registration No.: 801683017

Under the Supervision of

Dr. Gautam Setia

(Assistant Professor, Department of Mechanical Engineering)

DEPARTMENT OF MECHANICAL ENGINEERING

THAPAR INSTITUTE OF ENGINEERING AND TECHNOLOGY, PATIALA

July 2018

CERTIFICATE

I hereby declare that the thesis entitled "**Enhancement of Flow Properties and Flowability of Pharmaceutical Excipients (MCCP) and its Effect on Tabletability**" is an authentic record of my work carried out as requirements for the award of the degree of Master of Engineering in Thermal Engineering at Thapar institute of Engineering and Technology, Patiala under the supervision of **Dr. Gautam Setia**, Assistant Professor, Department of Mechanical Engineering, Thapar Institute of Engineering and Technology, Patiala during June 2017 to June 2018. No part of the matter embodied in this report has been submitted to any other university or institute for the award of any degree.

Date: 13th July, 2018

Krishang Kashyap

It is certified that the above statement made by the student is correct to the best of our knowledge and belief.

Dr. Gautam Setia
Department of Mechanical Engineering,
Thapar Institute of Engineering and Technology,
Patiala – 147004

i

Acknowledgements

I would like to acknowledge the research opportunity provided to me by **Thapar Institute and Engineering Technology, Patiala**. I am grateful for the funding provided by the institute for the procurement of the powders.

I am also grateful to my supervisor **Dr. Gautam Setia** for introducing me to the fundamentals of research. He provided me an excellent atmosphere necessary for the nurturing a research scholar to carry out his research. His advice had a deep impact on my analytical thinking and research work as well.

The results of the tabletability would not have been possible without the experimentation in **Chitkara University, Rajpura**. I owe great deal of appreciation to Dr. Sandeep Arora for allowing me to work in their campus.

I am also grateful to all the **researchers** who have worked before me without there insides this work wouldn't have been possible.

I am also grateful to the GATE scholarship provided by **Ministry of Human resource and Development (MHRD)** that allowed to carry out my research work.

Krishang Kashyap

Abstract

Flow properties of microcrystalline cellulose (MCC) excipients, Avicel PH 101 and Avicel PH 102 have been compared by using Brookfield PFT. Afterwards, the effect of hydrophobic Silica R972 as glidant has been tested on both the excipients. Hand blending is done by mixing MCCs with hydrophobic silica R972 vigorously by SAC as an underlined basis for 10 minutes and the flow properties tests are performed. During the flow function test "as received" Avicel PH 102 shows better flow function property as compared to "as received" Avicel PH 101. It was found that, with the increase in silica content there is a gradual increase in flow function of Avicel PH 102 silica blends whereas the Avicel PH 101 silica blends showed sudden increase in flow function which then lowered to negligible increase after 80% SAC. The wall friction angle of "as received" Avicel PH 102 shows lower values as compared to "as received" Avicel PH 101 while both showed a rise in wall friction angle with the inclusion of silica. However, bulk density of Avicel PH 101 first increases from 0% SAC to 60% SAC silica then decreases till 120% SAC silica. Whereas in Avicel PH 102, bulk density of silica blended samples have lower bulk density as compared "as received" Avicel PH 102. Tabletability is another parameter that has been compared by varying tablet mass (100 mg and 200 mg) and compaction force (0.75, 1 and 1.25 Metric ton). Tablets with more mass show higher strength and with increase in compactive force, there is increase in tablet strength. There is a decrease in tablet strength with increase in silica SAC.

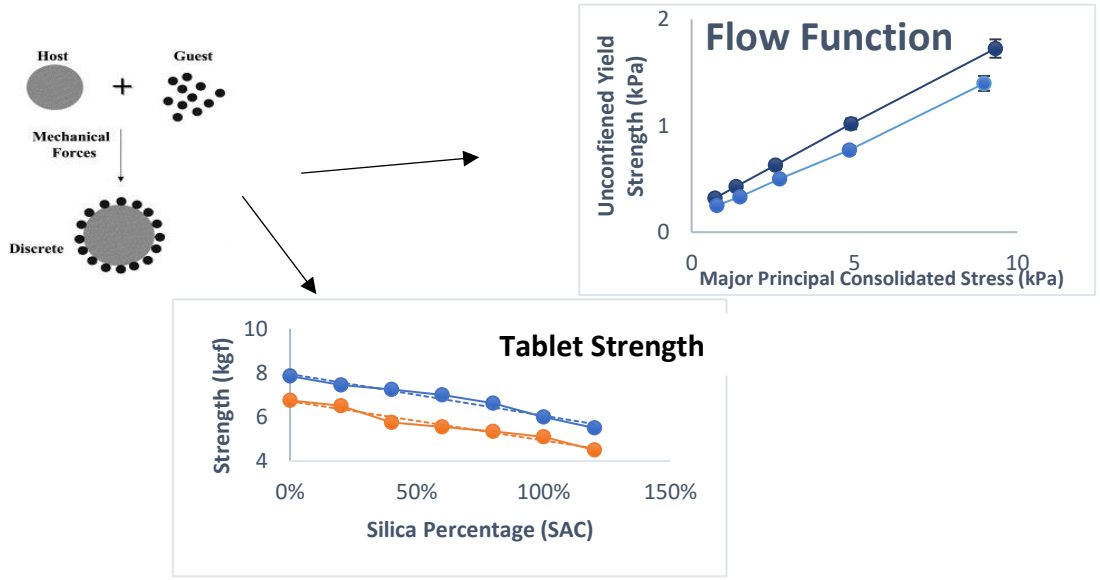

Keywords: Avicel PH 101; Avicel PH 102; Silica R972; Hand Mixing; Flow Function; Wall Friction; Tabletability

Contents

List of Figures

List of Tables

Nomenclature

dsv = Surface /volume ratio

d_a = Sieve Size

d_b = Front dia of gas bubble

d_{bi} = Initial bubble Size

h = Distance above Distributer

U = Superficial velocity of entering gas

U_0 = Minimum Fluidizing Velocity

N = Number of holes per unit area

g = Acceleration due to gravity

U_{mb} = Bubbling velocity

U_{mf} = Fluidizing velocity

K_{ms} = Units of s^{-1}

ρ_s = Density of particles

ρ_f = Density of Fluidizing gas

d' = Particle Size

z_0 = Dist. at which max. adhesion takes place

σ_{11}, σ_{22}, $\sigma_{\alpha\alpha}$ = apex of orign

σ = Mean of stresses

δ = effective friction angle

ε = Bed voidage

Θ = Hopper Half Angle

δ_j = Angle of internal Friction

ϕ_w = Mass flow limit of angle of wall friction

D = Mean particle diameter of excipient

d = Mean particle diameter of silica

N = Ratio of area of particles after and before blending

ρ_d = Particle density of R972

ρ_D = Particle density of excipient

Gwt% = Weight % of guest particle

SAC = Surface area coverage

ϕ = Angle of internal Friction

σ_n = Normal stress for a particular point

c = Cohesion

ρ_b = Bulk density of excipients

ρ_t = Tapped density of excipients

ρ_p = Particle density of excipients

Chapter 1

Introduction and Objectives

1.1 Introduction

The two components used in the pharmaceutical industry in the formation of any tablet are Active Pharmaceutical Ingredients (API) and Excipients. The combination of these two in definite proportions form the drug tablets. The process of formation of the final drug tablets involves dispensing of powder, powder blending, sizing, granulation and tablet compression. Inconsistent and poor flowability of powders is a problem that requires various troubleshooting mechanisms to make the powder flow again in pipes and hoppers for further processing. Flowability of different compounds varies due to various factors such as particle size, particle shape, particle size distribution, surface structure, surface energy, density, moisture content, chemical composition, temperature, pressure, fat content and anti-caking properties (Ganesan et al., 2007). Also, powders flow through different processes in pharmaceutical industry, which impart substantial changes in their physical properties such as powder density and flowability. Therefore, it is crucial monitoring these property changes to maintain good efficiency during the whole process of formation of tablets. Blockage can also take place due to powder agglomeration which can result to downtime in tablet manufacturing process. On the other hand, free flowing powders can cause flooding on the conveyor which is also undesirable because it compromises the product quality. Therefore, monitoring the powder flowability variations is required over each unit with precision (Koynov et al., 2015) and appropriate steps should be implemented ensuring the desired flowability of the powder is maintained. Flowability of different powders is measured by conducting a standardize laboratory test based on Jenike principle (Jenike, 1961; Schulze, 2008). The process comprises of generating flow function curves by calculating the flow function coefficient (Ripp et al., 2015). Flow properties are most commonly characterized by a shear cell experiment (Amagliani et al., 2016) for the design of hoppers as it is a tool widely used in the process of food and cement industry (Fitzpatrick et al., 2004). Unconfined yield strength, angle of internal friction and cohesion are also determined by analysing the Mohr's circle generated through the flow function test (Bian et al., 2015).

However, it seems that the information on the application of flow function in the pharmaceutical powders is limited in open literature. On the other hand, maintaining the pre-deterministic powder flowability is requisite for the quality control of the drug. For high speed tableting fixed values of flow properties must be maintained (Dudhat et al., 2016). Glidants are being used at an increasing rate in the pharmaceutical industry to reduce powder agglomeration and to increase flowability (Tremantozzi et al., 2017). It is reported that glidants used in excess, hampers surface morphology (Morin et al., 2013) and reduces tablet strength (Chen et al., 2018). Therefore, the surface area coverage of glidants over the host particle must be carefully selected so that flowability should not increase to an extent that it will adversely affect tabletability.

The need of this study is to examine the effect hand blending based surface modification as a viable approach towards developing high functional excipients which have better flow characteristics, packing density and high compactability. For this purpose, MCCs Avicel PH 101 and Avicel PH 102 are compared with the help of Brookfield PFT on as received basis. Hand blending is done by mixing MCCs with hydrophobic silica R972 vigorously by SAC as an underlined basis for 10 minutes and the flow properties tests are performed. In the field of drugs, the process of tablet formation is an essential part of drug formation. Therefore, tablet strength is the parameter which is essential for investigation as glidant (silica R972) is added to the parent MCC excipient powder. The evaluation of tabletability and tablet strength is necessary.

In this dissertation, flow properties and flowability of excipients Micro Crystalline Cellulose (MCC) specifically Avicel PH 101 and Avicel PH 102 are investigated. The comparison between there flow function coefficient, wall friction angle, angle of internal friction, bulk density and tablet strength is done. For glidant, the nano-sized compound hydrophobic silica R972 is selected. Silica R972 is hand blended with both the excipients with varying surface area coverages of 20%, 40%, 60%, 80%, 100% and 120% and the improvements in the flow properties are compared with their respective parent excipient compounds. Tabletability is another parameter which has been compared between different excipients and silica blended mixtures. By varying the tablet mass and compaction force (0.75, 1 and 1.25 Metric Ton), tablet strength has been compared.

1.2 Objectives

This thesis is focused on measuring flow properties with the help of Brookfield PFT. Specific objectives include:

- To investigate the flow properties of “as received” Avicel PH 101 and Avicel PH 102 excipients using Brookfield PFT.
- To investigate the improvement in flow properties by virtue of blending of nanosized hydrophobic silica R972 based on different surface area coverage with above mentioned MCCs with the help of Brookfield PFT.
- To investigate the effect on Tabletability of all the different hand mixed blends (Avicel PH 101 and Avicel PH 102) with R972 silica as per SAC.

Chapter 2

Literature Review

In this chapter, the theory of powder fluidization, flow properties and tabletability of bulk solids are discussed. The theory behind the shear cell testing of powders is explained. Powder flow tester used for the obtaining the results is explained. The parameters required for the calculation of tablet strength has been discussed. Finally, the work of different researchers leading up to this work has been reviewed.

2.1 Mohr Circle Analysis

Virtually every industry requires bulk solids in some form or another. Either the bulk solid is being transported from one place to another or it is being dropped timely with the help of a hopper. Bulk solids comprise of particles that have a particle size of 2 mm or less. Under certain conditions they exhibit properties of both solids and liquids. Bulk solids consolidate when compressed or left untouched for a certain amount of time. This behaviour of bulk solids can be observed in a heap of sand which belongs to Geldart B particle group (Geldart, 1973). Powders are combination of bulk solids, gases (as interstitial voids) and liquids (as moisture) that creates complexities in its analysis (Lumay et al. 2012). The Lagrangian approach of particle-particle interaction is difficult and the results formed have less practical applicability. Therefore, Eulerian approach has been adopted by many researchers where empirical relations have been formed to describe the behaviour of the powder based on the experimental results. Following this approach bulk solids are studied by subjecting them to different load conditions. For this calculation, the first shear cell was invented by A W. Jenike (1964) for powder flowability assuming powders as pseudo solids.

It has been found that, to analyse the flow of bulk solids they can be assumed as pseudo solids and theory of two-dimensional Mohr circle can be applied on it.

As the compressive vertical stress σ_v is applied on the powder and the powder containment area is confined, the horizontal stress σ_h is generated, as shown in Figure 2.1.

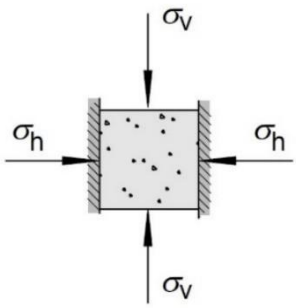

Fig 2.1: Element subjected to vertical and horizontal stress (Schulze, 2008)

The horizontal stress is always less than vertical stress. Usually the horizontal stress ranges from 30-60% of the vertical stress. Both vertical and horizontal stresses are assumed as principle stresses in case of frictionless container walls. As the powder flows through the container, in practical scenarios shear stress is also introduced due to friction along the wall of the cylinder.

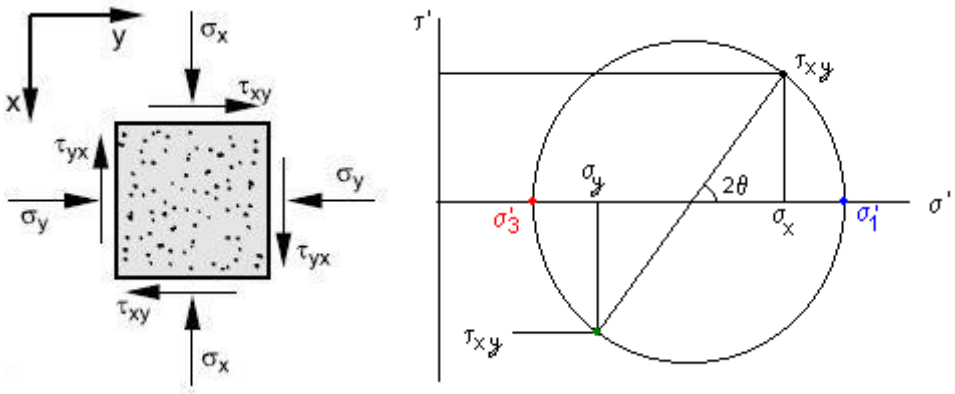

Fig 2.2: Equilibrium of forces and corresponding Mohr Circle (Schulze, 2008)

The equations governing the normal stress and shear stress at an any arbitrary angle is given by:

$$\sigma_\Theta = \frac{\sigma x + \sigma y}{2} + \frac{\sigma x - \sigma y}{2} \cos 2\Theta + \tau_{xy} \sin 2\Theta \qquad (2.1)$$

$$\tau_\Theta = \frac{\sigma x - \sigma y}{2} \sin 2\Theta + \tau_{xy} \cos 2\Theta \qquad (2.2)$$

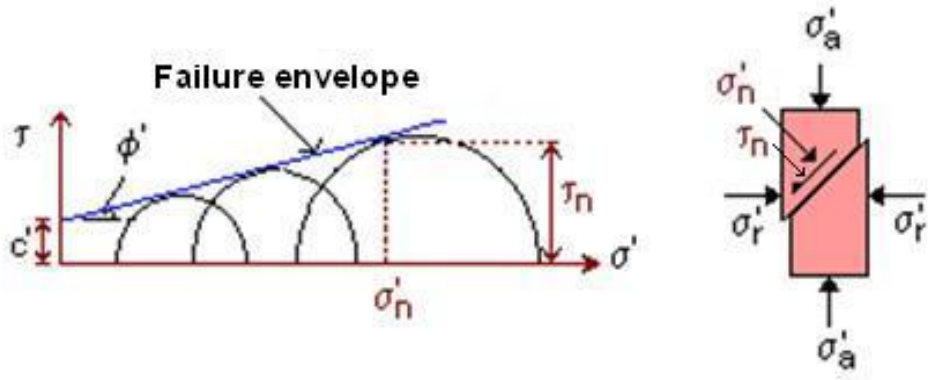

Fig 2.3: Failure locus over increasing stress levels (nptel)

In solids, the locus of yielding passes through the point of origin. This yield locus is tangential to the Mohr circle generated by the unconfined yield stress and the consolidating stress. But in bulk solids the y-axis intercept does not take place at the origin, rather it takes place in the positive y-axis and this distance between the point and the origin is called as cohesion. The yield locus of bulk solids is not a straight line, the locus shows hogging or sagging (depending upon the powders selected) at lower stress levels. This behaviour is neglected during bins and hoppers designing. The equation governing the shear stress (at low stress) values is given by:

$$\tau = \sigma_n \cos\phi + c \qquad (2.3)$$

This equation provides the shear stress required for the failure of the bulk solid at a particular normal stress.

2.2 Shear Cell Tester

For the implementation of Mohr circle principle, the instrument used is shear cell tester.

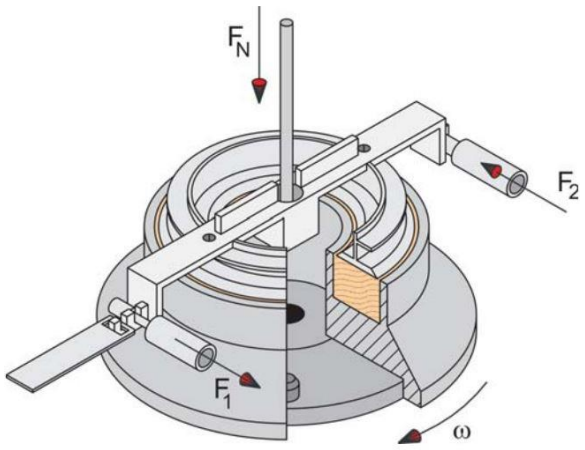

Fig 2.4: XS-Mr type Ring shear cell (Jenike.com)

Initially designed by Jenike (1964) for the calculation of the flow properties of a mass flow system. Shear cell tester requires the peripheral confinements of the shear tester to be detached after consolidating the powder, which became a bottleneck in the testing. Keeping a constant bulk density and homogeneity in the bulk material is difficult while keeping low shear. In recent times, the type of shear cell tester used is annular type which imparts a shear force onto the consolidated powder to compensate the removal of the bulk solid confinements. This lets the different layers of the powder to break and slide over each other. There are various types of annular shear testers such as FT4 Rheometer, RST-XR Schulze Ring Shear Tester and Brookfield Powder Flow Tester. In translational shear tester the total deformation is limited while keeping the properties of the powder constant, but the ring shear tester can perform large deformations. It is the main advantage of ring shear testers, that is why they are more prevalent. In this dissertation, the tester used is Brookfield Powder Flow Tester (PFT) designed by AMETEK Brookfield. The maximum powder diameter acceptable for the experimentation is 2mm with 90% of the particles below 1mm size.

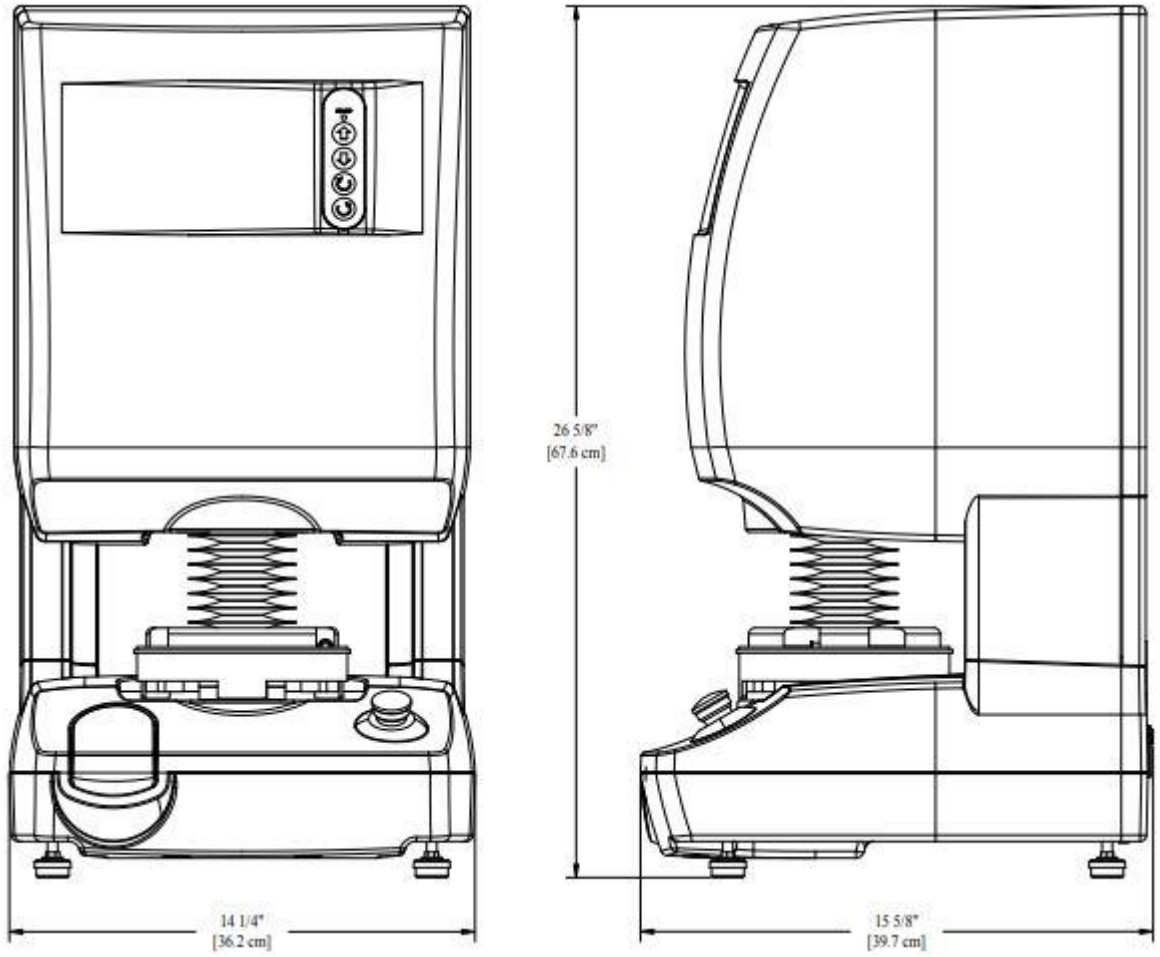

Fig 2.5: Depiction of Brookfield PFT (PFT Manual)

The properties that can be calculated through this machine are as follows:

- Unconfined failure strength
- Major Principal Consolidating Stress
- Time Consolidation
- Angle of internal friction
- Angle of wall friction
- Cohesive strength
- Bulk density

Flow Function – According to A.W. Jenike (1964) it is the ratio between unconfined yield strength and consolidated stress. This shows how much easy or difficult is it for the powder to break its adhesion and flow through the hopper.

Smaller value of flow function exhibits to better flowability of the powder through the hopper. Flow problems that are associated with flowability of bulk solids such as arching and ratholing can also be identified by this property (Ripp et al., 2015).

Time Consolidation Test – This test is similar to flow function test but here the powder is left untouched for a lot of time. This gives powder some time to self-adhere which increase the stresses required to break the powder adhesion (Fitzpatrick et al., 2004).

Wall Friction test – The friction between the powder and the wall which hinders the flow and causes either mass flow or funnel flow to take place. Wall friction test is such a test which takes this parameter in check. This test provides the effective wall friction angle (°) by which the wall is applying force on the powder (Iqbal et al., 2006).

Bulk Density – It is also an important property that helps in the in the identification of amount of compression taken place in the bulk solid under load.

The tests performed on the machine are standard flow function test, standard wall friction test and standard bulk density test. The time consolidated flow function test has been omitted after discussion with the industry, because nowhere in the whole process line the powders are kept stationary for such a long period of time except packaging. If the powder is packaged and sent to another factory for further process the powder is taken out from the bag manually which cancels the requirement of finding the time consolidated flow function results.

The basic walkthrough of the process of testing is as follows:

- Connect the machine to the powder flow tester application on the computer and link them.

- Select the trough over which the powder has to be placed. Weigh the powder and place it in the trough by passing it through a sieve, depending on the type of test to be done using the shaping blade create either a curved profile for flow function tests or a flat profile for both wall friction and bulk density tests.
- In the Powder flow tester place either the vane type lid for flow function tests or a flat lid for both wall friction and bulk density tests and place the trough below the lid.
- Now in the application select standard/custom test option and select the type of the type of test to be performed. During custom tests choose the desired parameters.
- Place the weight of the powder and start the test.

The tester then performs a series of normal and shear forces with the algorithm running at the back end, solves certain equations and provides the plot for property selected.

2.2.1 Flow Function Test

This is the primary test that must be performed to know about the flowability of the bulk solid. Figure below depicts the sequence of conditions that must be created to obtain the flow function.

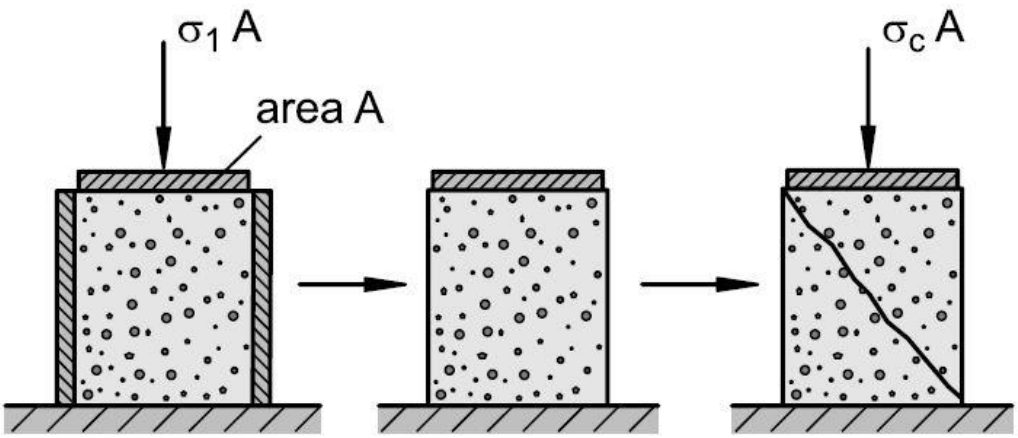

Fig 2.6: Yield Failure in bulk solids (Schulze, 2008)

This method is used in Jenike shear tester. The process starts by first placing the powder in a top open container. Then by using a plunger applying a certain amount of stress from the top, and this stress is called major principal consolidated stress (σ_1). Now remove all confinements and over the top use the plunger to apply more stress till the powder breaks this stress is called unconfined yield stress (σ_c). By increasing the major principal consolidated stress we obtain a certain tend which when plotted provides the flow function (ff_c). Flow function is the ratio of

major principal consolidated stress and unconfined yield stress. Flow function signifies how easy is flow powder to break consolidation and flow again. There are 5 regions of flowability which provides an idea of powder flowability (Schulze, 2008).

- Non-flowing Region $ff_c < 1$
- Very Cohesive Region $1 < ff_c < 2$
- Cohesive Region $2 < ff_c < 4$
- Easy Flowing Region $4 < ff_c < 10$
- Free Flowing Region $10 < ff_c$

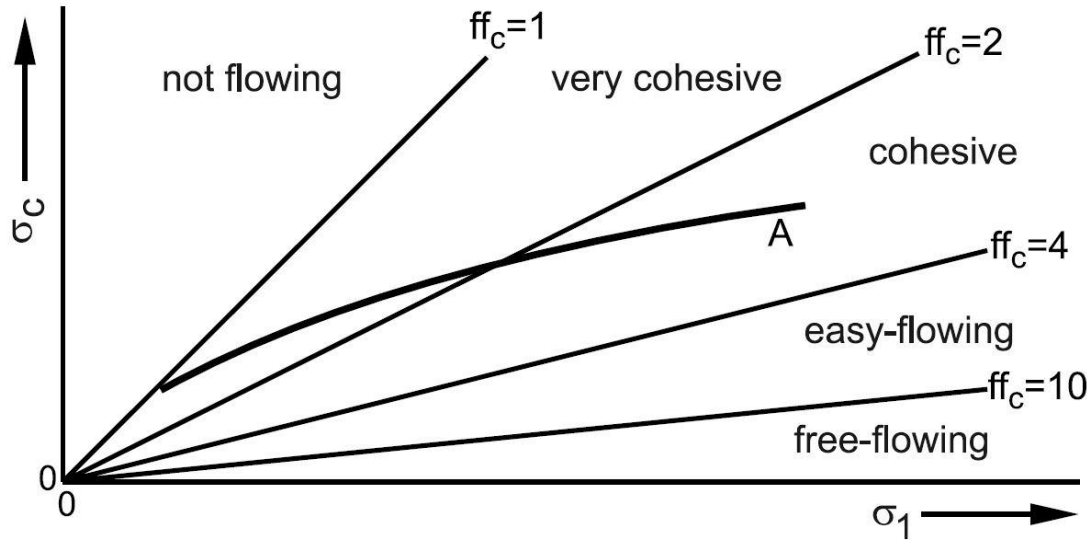

Fig 2.7: Flow Behaviour Regions (Schulze, 2008)

There is no removal of confinements in the Brookfield PFT. Therefore, torque is used instead to obtain the above results. To identify one point to plot, the Brookfield PFT firstly consolidates and then breaks the powder at peak stress/Consolidated Stress (CS). Then applies the same process at stress values CS/3, 2*CS/3 and CS. The trend line joining these points provides the flow function curve.

2.2.2 Wall Friction Test

The friction between the powder and the wall which hinders the flow and causes either mass flow or funnel flow to take place. Wall friction test keeps this parameter in check. This test provides the wall friction angle, which is the angle at which wall is applying force on the powder (Iqbal et al., 2006). The parameter noted in this test is effective angle of wall friction

(ϕ). As the effective angle of wall friction angle increases, friction due to wall also increases (Iqbal et al., 2006). Therefore, as the friction angle increases, more force is being applied horizontally onto the wall and less compaction is taking place in the powder as shown in the following equation (Schulze, 2008).

$$\sigma_1 = \frac{\rho g D}{4k\ tan\phi}\left(1 - e^{\frac{4k\ tan\phi z}{D}}\right) \quad (2.4)$$

where,

σ_1 = Major Principle Consolidating Stress (kPa),

k = ratio between vertical and horizontal stress (kPa),

z = powder depth (m),

D = diameter of silo/hopper (m), and

ρ = bulk density (kg/m^3)

2.2.3 Bulk Density Test

With increase in bed height, weight of the bulk solid increases. This increase in weight self-compresses the bulk solid. The reason this test is practiced, is to know how much powder compresses under load and its impact over powder flowability. If the bulk density change in the powder is not significant, the powder tends to show less compressible behaviour.

2.3 Previous Work on Flow Properties

Jenike (1987) analysed the flow in a hopper. The stress equation associated with the flow is shown-

$$(\sigma_{11} - \sigma)^2 + (\sigma_{22} - \sigma)^2 + (\sigma_{\alpha\alpha} - \sigma)^2 - 2\sigma^2 sin^2\delta \quad \text{[Tresca Theory]} \quad (2.5)$$

$$\sigma_{11} \leq \sigma_{\alpha\alpha} \leq \sigma_{22} \quad (2.6)$$

$$0 \leq \delta \leq 60 \quad (2.7)$$

$$sin\delta = 3^{0.5}\ (\sigma_{11} - \sigma_{22} / 2\sigma_{11} + \sigma_{22}) \quad (2.8)$$

Stress and strain deviatorics are formulated, differential equations are derived for both cone and pyramid flow and the flow is compared.

- Effective angle of friction is calculated through stresses in a perpendicular section.
- Strain rates are calculated with respect to velocity of radial motion.
- Velocity profile is calculated.
- Compressibility is calculated as change in log of density over change in the log of stress difference.

Wouters et al. (1996) took a different approach to deduce the flowability of powder. Angle of repose is calculated for both group C and group A powders and comparison is done with respect to particle size and Hausner ratio. Powders with low angle of repose show an inverse relation with low mean particle size i.e. low mean particle size powders have high angle of repose.

Gabaude et al. (2001) compared different pharmaceutical powder. The powders compared are Avicel PH 102, Starch 1500, Pharmatose DCL, starch and Lactose. In this paper, particle size distribution of all the powders is made to know to identify which Geldart group the powder belongs to. Tapped and aerated densities are calculated and their respective Hausner ratio and Carr index are calculated. Flow function of the powders are calculated which showed every powder is in easy flowing region while lactose shows free flowing behaviour.

Mercury intrusion porosity test is also performed which is used to calculate the porosity in the powder, bigger size of mercury bubble attribute to more porosity. Avicel PH 102 showed the highest porosity at 1.8 while starch and lactose showed the minimum porosity at 0.5 and 0.7 respectively.

Ganesan et al. (2008) described the flowability of bulk solids and its handling characteristics with respect to various factors. These are moisture content, humidity, temperature, pressure, particle size, flow conditions and anticaking agents, angle of repose, bulk density, frictional forces and compressibility.

Moisture content increases the cohesiveness of the powder. With more moisture van der Waal force increases, and the powder does not fluidize. At high moisture group A powder can behave like group C and do not fluidize. Humidity has a similar impact over powder, increasing humidity lowers the flow function which is not desirable. Increasing temperature also increases the cohesiveness of the powder and freezing it allows ice to form and bond with the particles which again hinders the flow. Thereby the desirable temperature of operation is required which is at room temperature.

Pressure attributes to two phenomena. Firstly, in the compaction of the powder which makes adhesive bonding between the particles and secondly, critical arching which hinders the flow. Thereby some pressure is required but over pressure is undesirable.

Particle size and distribution plays a very vital role in fluidization. If particle size decreases, it shows resistance to flowability. Bigger size particle shows higher compressibility which is required for tabletability.

Bulk density is also an important component of criteria over which the powder flow is determined. It directly attributes to the flow the powder inside the hopper wall (Johnson 1971/1972) its impact over powder flow is to be checked as the flow happens.

Morin et al. (2014) compared the mixture of metallic lubricant powders in w/w ratio with API. Mixture of magnesium stearate, magnesium silicate, calcium silicate and steric acid with lactose are compared. Angle of repose in magnesium stearate blend showed a decline till 1.5% of inclusion then remain constant. In magnesium silicate blend, AOR declined till 2% inclusion then remains constant, in calcium silicate blend, AOR first decreases till 0.3% inclusion and then increase as calcium silicate percentage increases, and then AOR becomes constant at 3% inclusion. In steric acid addition the blend shows the same behaviour as magnesium silicate and becomes constant at 2% inclusion.

Macri et al. (2016) calculated the flow properties of synthetic and natural rutile and observed the powders at room temperature 25^0C and high temperature 500^0C. Flow function of NR25 and SR25 are lower than NR500 and SR500 respectively. Flow function NR25, SR35 and NR50 are in free-flowing region whereas SR500 flowability is in easy flowing region i.e. it possesses more resistance to flow with respect to natural rutile at both 25^0C and 500^0C and synthetic rutile at 25^0C. This shows as the temperature to the powder increases it is more difficult for the powder to flow from the hopper.

2.4 Powder Classification

It is required to understand the physics that governs the flow of the powder, so as to engineer the most efficient way to transfer and use the product. A way of transferring the powder without adding any additional cost to manufacturing chain is to pneumatically convey the powder. This eliminates the process of making a slurry and evaporating the water after transport. The physics governing this flow is to be deduced, and when the powder enters in a hopper there are stresses that act on the particles that behaviour is to be examined.

There are 4 broad groups with which powder flow in pipes can behave like i.e. Group A, B, C and D as explained by (Geldart, 1972). These are made based on mean particle size, change in bed height, bubble size, density of the powder and expansion ratio of the powder.

Based upon the above study a classification diagram is made between mean particle size and fluidizing air density difference, as shown in figure 2.8 (Geldart, 1973).

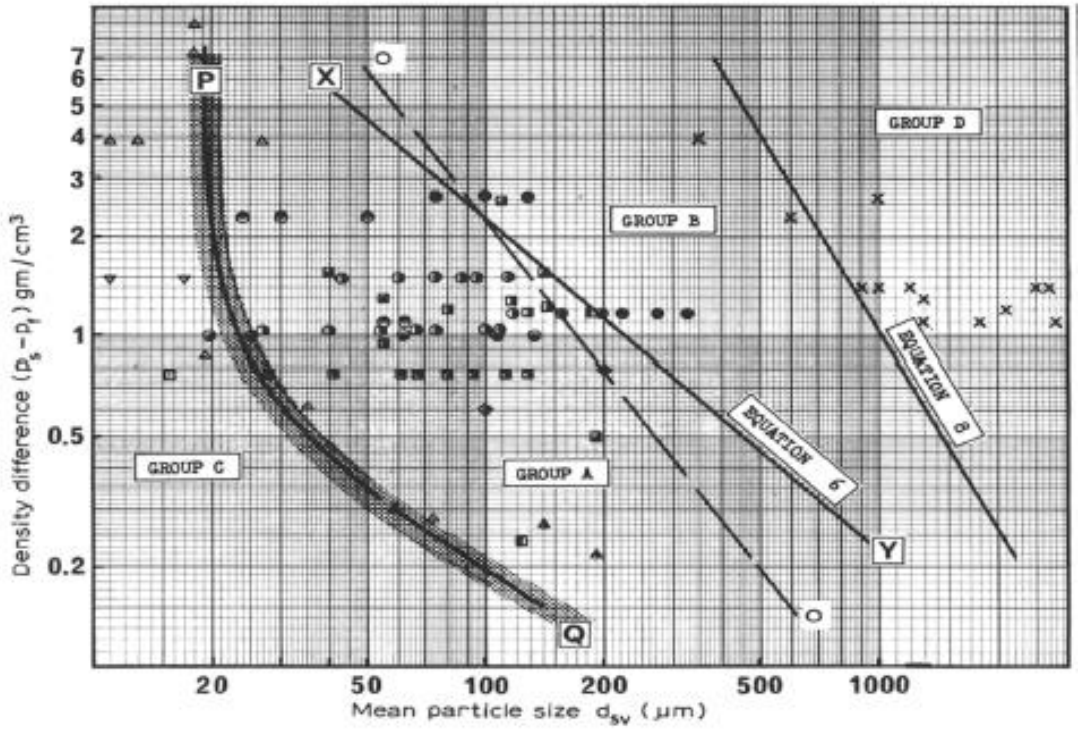

Fig 2.8: Powder classification diagram for fluidization by air (Geldart, 1973)

2.5 Previous Work on Powder Classification

Geldart (1972) describes the individual groups in which each powder can be grouped. These vary by particle size, fluidizing pressure and bubble size which are followed by the equations as follows-

Particle size $$d_{sv} = 1/\Sigma(x/d_a) \quad (2.9)$$

Bubble size $$d_b = d_{bi} + k\, h^{p1}(U - U_0)^{p2} \quad (2.10)$$

$$d_{bi} = \{1.43\{(U - U_0)/N\}^{0.4}\}/g^{0.2} \quad (2.11)$$

Group A: Particle Density < 1.4 g/cm^3

Size range = 20-100 μm

Dense phase expansion takes place i.e. the whole bed expands before any visible bubbling and bed collapse is at a constant rate around 0.5-1 cm/s.

Group B: Particle Density = 1.4-4 g/cm^3

Size range = 40-500 μm

Bubbling starts as soon as the gas velocity hits the minimum fluidisation velocity. There is small bed expansion before bubbling starts and when the supply of air is cut off the bed collapses immediately.

Group C: Size range < 30 μm

These particles are very sticky and contain moisture in them. As the air is passed the bed height increases till an extent then collapses down. Channels are formed in the powder from which air passes.

Group D: Particle size > 600 μm

Bubbles are formed as the pressurised air is passed but the velocity of the bubble is slower than the interstitial gas velocity so the bubbles collapse on themselves.

Geldart (1973) describes the variations in the groups as a function of density difference, initial velocity of free air and bubbling velocity of air and found

For Group A and B

$$U_{mb} = K_{ms}\, d_{sv} \qquad (2.12)$$

$$U_0 = \{0.008 d_{sv}^2(\rho_s - \rho_f)\}/H \qquad (2.13)$$

$$(\rho_s - \rho_f)\, d' \leq 225 \qquad (2.14)$$

For group B and D

$$(g\, d_b/2)^3 \leq 0.008 d_{sv}^2(\rho_s - \rho_f)\, g\}/H\, \varepsilon_0 \qquad (2.15)$$

$$(\rho_s - \rho_f)\, d'^2 \geq 10^6 \qquad (2.16)$$

In group A bed height increases at minimum fluidization velocity and as the velocity increases bubbling takes place. Group B particles show bubbling at minimum fluidization velocity. Group C particles don't fluidize at all, they initially increase the bed height and then as fluidization velocity increases they form cracks and creates channels for the air to flow. Group D particle sprout with very big bubbles and they do not fluidize but if we increase the area of the bed they behave like group B particles.

2.6 Tabletability

Tabletability is the relation between compaction force and tablet strength. Based on the pioneering work of Fell and Newton (1970), relation for the calculation of tablet tensile fracture stress (TTFS) is developed. The relation is given by the following relation:

$$\sigma = \frac{2F}{\pi D t} \qquad (2.17)$$

In practice, TTFS is measured by simply placing the tablet vertically and very slowly applying diametrical load on it, as shown in the figure 2.10.

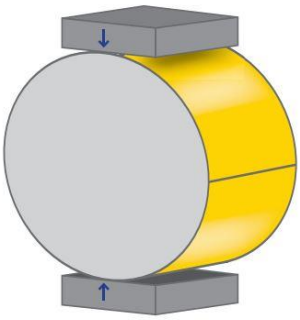

Fig 2.10: Assessing the compaction behaviour of orally dispersible tablets (tabletcapsules.com)

The materials that result in the strongest tablets at a certain pressure, usually show better tabletability property. This is because, the tablet that can be produced at the lowest compaction force is also easier to manufacture. Measuring tabletability has been recognized as a simple, effective and highly sensitive way to characterize and compare compaction properties of powders.

Therefore, it is required to understand the effect of flow enhancements over tabletability. Generally, as the flow of powders tend move on the free-flowing region, it becomes difficult for the powder to have a good tablet strength. As the size to the particle increases there is a reduction in tabletability (Sun et al., 2006).

2.7 Previous Work on Tabletability

Chen et al. (2018) investigated the flowability and tabletability of Avicel 105, Avicel PH 101 and Avicel PH 102. Glidants used are A200, R972 and M5-P. Avicel 105 is dry coated through Resonant Acoustic Mixer. Scanning Electron Microscopy, Particle Size Distribution, powder characteristics through FT4 and tableting performance tests are conducted.

Bulk density (BD) increases from uncoated Avicel 105 to blended Avicel 105 with 1% A200 to DC Avicel 105 with 1% A200. Flow Function (FF) increases from uncoated Avicel 105 2.53 to blended Avicel 105 with 1% A200 3.8 to DC Avicel 105 with 1% A200 21.9.

Compaction is reduced from uncoated Avicel 105 9.3MPa to DC Avicel 105 with 1% A200 7.8MPa. Dry coating of Avicel 105 with A200, M5-P and R972 achieves maximum flowability and bulk densities with only 10% reduction in compaction. The amount of silica chosen is 0.7% as the limit is 2%.

Chen et al. (2018) investigated the tabletability characteristics of Avicel PH 102 as the host powder with guest particles A200 and R972. Pre-mixing is done by V blender and dry coating done by fluid energy mill.

Flow function of Avicel PH 102 with coated silica shows better results than uncoated Avicel PH 102, and A200 coated powder shows better flowability than Avicel PH 102 with R972 coating.

Bulk density increases with inclusion of silica. Avicel PH 102 with R972 coating has less bulk density as compared to A200 coated powder. Compactability decreases with increase in porosity and increases with increase in compaction pressure.

Tensile strength (TS) of silica coated powders is less than uncoated Avicel PH 102. Avicel PH 102 with R972 coating has the least tensile strength. Both the experiments show increase in FF

and BD and reduction in TS but A200 has less compaction reduction and more TS with respect to R972.

2.8 Previous Work in Thapar Institute

Rohilla et al. (2016) measured the flow properties of different fly ash obtained from seven ESP field hoppers. The evaluation of mass flow and funnel flow vessels for the critical dimensions have been investigated using flow properties of the powder. Cohesion has been modelled and compared against the yield strength of fine powders of different flowability. The fly obtained from the first four stages show a n easy flowing behaviour whereas later stages show cohesive flow. The aeration rate required for the flow have been obtained based on minimum fluidization velocity and permeability factor. A new model of cohesion has been generated that does not require the need of calculation of the shear testing of the powders and provides the ~20% accurate results to the existing models.

Vivek et al. (2017) investigated the flowability of 6 Pharmaceutical (2 API and 4 excipients) powders and one detergent powder are investigated. Parameters compared between the powders are flow function, wall friction, bulk density and hopper half angle. Arching, inadequate flow (funnel flow) and rat holing has been investigated. Powders have been classified on the basis of flowability which shows lactose very cohesive flow, starch having cohesive flow and detergent showing cohesive behaviour. Hopper dimensions of paracetamol, calcium sulphate, detergent and magnesium Tri-silicate show high exit dimension.

Chapter 3

Materials and Methodology

3.1 Introduction

In this chapter, the details for the procurement of different compounds, methodology behind blending, calibration of the shear tester and different tests performed are provided. The details of the results are in succeeding chapters.

3.2 Materials/Powders

In the study, the MCCs studied are Avicel PH 101 and Avicel PH 102. The procurement of Avicel PH 101 is from Signet Chemical Corporation, USA and of Avicel PH 102 is from JRS Pharma, USA. All the samples have been tested on as received basis.

The flow properties and tabletability of these compounds have been compared by hand blending with glidant. The powder used for this purpose is hydrophobic nano-silica R972 which has been procured from Kanchan Rasayan, Mumbai. It has been specified in Food and Drug Administration (2009), the acceptable limit of glidant blending/coating in any drug is ~2 wt %. The combinations of R972 and excipient blends selected are at SAC percentage of 20, 40, 60, 80, 100 and 120 as its weight percentage at 120% SAC is under the 2 wt % limit.

The method of mixing excipients and glidant is by taking cumulative weight of 50g, where (x)g of glidant is added to (50 – x) g of excipient. They have been mixed thoroughly for 10 minutes and then the tests have been undertaken.

3.3 Physical properties measurement

The physical properties of bulk solids include particle shape, particle density, Hausner ratio, Carr index and bulk density. Description and testing method about the above terms has been provided below.

3.3.1 Bulk, Tapped and Particle Density

Bulk density (ρ_b) is measured by taking a specified mass of powder in a measuring cylinder and dividing it by the volume it occupies. This property varies a lot depending upon various conditions such as moisture content, packing, compaction and compressibility.

Tapped Density (ρ_t) is measured by tapping the cylinder containing the bulk solid and then dividing it by its residual volume. During the experimentation, each sample was tapped 500 times to obtain the tapped density.

Particle Density (ρ_p) is measured by water displacement method. Specified amount of water is poured in the measuring cylinder and its volume is measured. The excipient weight is measured, and they are suspended in the water and the volume of the mixture is measured. Particle density is the ratio of the mass of the particles added to the change in volume.

Parameter calculated with these measurements are:

- Porosity (Li et al., 2016)
- Compressibility Index (Ji et al., 2017)
- Hausner Ratio (Grey and Beddow, 1969)

$$\text{Porosity} = 1 - (\rho_b/\rho_p) \quad (3.1)$$

$$\text{Compressibility Index} = 100 * [1 - (\rho_b/\rho_t)] \quad (3.2)$$

$$\text{Hausner Ratio} = \rho_t/\rho_b \quad (3.3)$$

Hausner ratio is the ratio between tapped density and bulk density (Grey and Beddow, 1969) as reported in Geldart et al. (2006) and Guo et al. (1985). Geldart diagrams classify powders on the basis of Hausner ratio as HR > 1.25 belongs to Geldart group A, 1.25 < HR < 1.4 belongs to an intermediatory state of A/C i.e. these particles show the properties of group A and group C and HR > 1.4 belongs to Geldart group C.

3.3.2 Scanning Electron Microscopy (SEM)

Scanning electron microscopy (SEM) images have been obtained from the Sophisticated Analytical Instruments (SAI) Laboratory, Thapar Institute of Engineering and Technology, Patiala. The powder has been placed on carbon tape over an aluminium stub and coated with gold and palladium (80:20 ratio) in JSM-5510. SEM manufactured by JEOL Ltd.

3.3.3 Particle Size Distribution (PSD)

The particle size measurements have been made by Laser Diffraction method through Mastersizer 2000 (Malvern Instruments Ltd, Worcestershire, UK) at Choksi Laboratories Limited 829 GIDC Makarpura, Vadodara, Gujarat. The measurements noted are d_{10}, d_{50} and d_{90}. The subscripts indicate the percentage of particles having less than that certain diameter.

3.4 Annular Shear Tester

3.4.1 Powder Flow Tester

Brookfield Powder Flow Tester (PFT) manufactured by AMETEK Brookfield at Laboratory in Particle and Bulk Solid Technology Laboratory, Thapar Institute of Engineering and Technology, Patiala. It is an annular shear tester in which powder is filled in a 6-inch perforated trough PFT – 405 and placed in the machine, then compressive stress is applied on the powder. The shear cell lid rotates at a computerized angular velocity to shear the consolidated powder. There are two lids for the measurement of properties. These are (i) vane type lid PFT - 515 which is accompanied by an inner catch tray with curved profiler for the flow function test, and (ii) wall lid PFT - 516 which is accompanied by inner catch tray having flat profile for wall friction and bulk density tests.

Fig 3.1: Powder flow tester (PFT Manual)

The instrument operates with the help of Powder Flow Pro software which computes the readings obtaining from the instrument. Places the values in the formulae accompanying the software and provides the trends of flow function, wall friction, bulk density and hopper half angle. The software also provides other vital parameters such as cohesion and angle of internal friction.

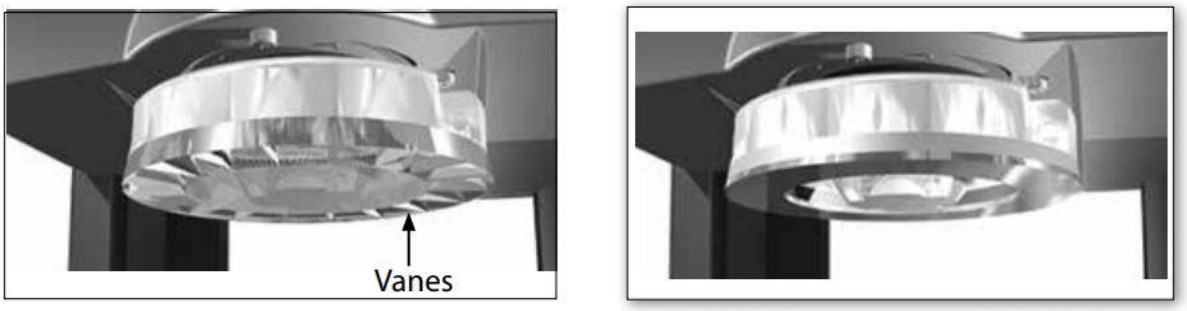

Fig 3.2: Flow function and wall friction lid (PFT Manual)

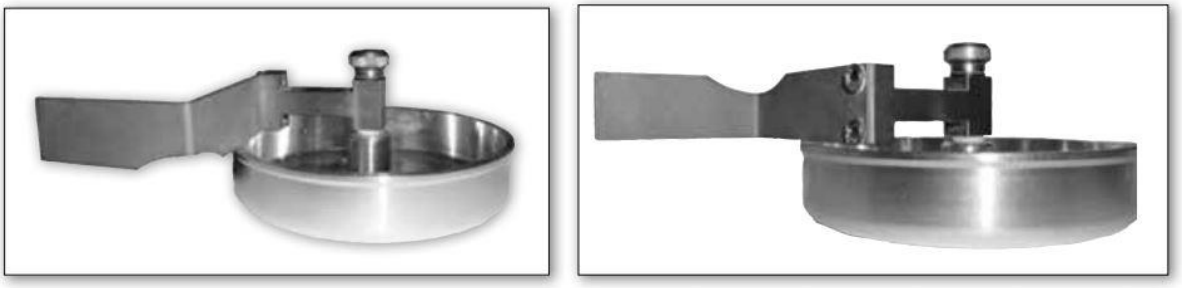

Fig 3.3: Flow function and wall friction shaper trough (PFT Manual)

3.4.2 Operating Procedure

Procedure for the flow function test is as follows:

- Using a spirit leveller. adjust the screws at the base of the tester.
- Turn ON the power supply and connect the instrument to the PC with the Powder Flow Pro software.
- Go to the setup tab and click on connect.
- Weigh the trough and calibrate the weighing machine to zero (0).
- Pour the powder in the trough using a sieve and create the curved profile using scratching tool over the inner tray catch.
- Weigh the trough again and note the weight.
- Setup the instrument with the flow function lid and place the trough under it.

- Open the test section inside the Powder Flow Pro software and provide the batch name, powder name and the weight of the powder in grams.
- Select the standard/custom testing method and select the desired test. Under the custom test, change of the fine details is also possible.
- Click “Run Test” in order to run the test.
- Save the result after the completion of the test.
- By using the buttons provided on the instrument remove the trough.

Procedure for wall friction and bulk density test is as follows:

- The process for these tests is almost identical to the above process barring some key points.
- The lid used in these tests is the flat lid and the scrapping tool used in the sample formation is also flat corresponding to the lid.
- In the selection of test in the Powder Flow Pro software wall friction test or bulk density test has to be selected.

3.5 Flow properties measurements

3.5.1 Flow function curve

Yield locus of bulk solids is formed by breaking the bulk solid under a specific consolidated stress (σ_1) by applying shear stress on the sample (Schulze, 2008). Yield locus is the curve formed by measuring the yielding on five different consolidating stresses. In bulk solids there is already some stress, there is requirement of some shear stress to make the powder flow even at zero normal load. It is due to the self-weight of the bulk solid compressing the powder. The shear stress intercept obtained on the y-axis is called cohesion (C) (Schulze, 2008). The equation governing the shear stress is as follows:

$$\tau = \sigma_n \cos\phi + c \qquad (3.4)$$

where,

ϕ = Angle of internal friction (degree),

σ_n = Normal stress for a particular point (kPa), and

c = Cohesion (kPa)

The yield locus of excipient Avicel PH 101 is shown in Fig 3.4. The locus has been formed by consolidating the powder at different pre-shear stresses which increase in a geometric progression. The different pre-shear stress through which the yield locus has been formed are 0.301 kPa, 0.602 kPa, 1.204 kPa, 2.409 kPa and 4.819 kPa which are represented by stress 1 to stress 5.

Fig 3.4: Yield locus of a sample of Avicel PH 101

These yield loci are used to form the flow function curve between unconfined yield strength (σ_c) and major principle consolidated stress (σ_1) as reported in Schulze (2008). As per Jenike (1964) the flow function area is divided in 5 regions. These are as follows:

- Non-flowing Region $ff_c < 1$
- Very Cohesive Region $1 < ff_c < 2$
- Cohesive Region $2 < ff_c < 4$
- Easy Flowing Region $4 < ff_c < 10$
- Free Flowing Region $10 < ff_c$

Other properties which are obtained from the flow function curve are effective angle of internal friction and cohesion. These properties are also an indicator of the ease of flow. Generally, as the effective angle of internal friction and cohesion decreases, the powder tends to be in free-flowing region.

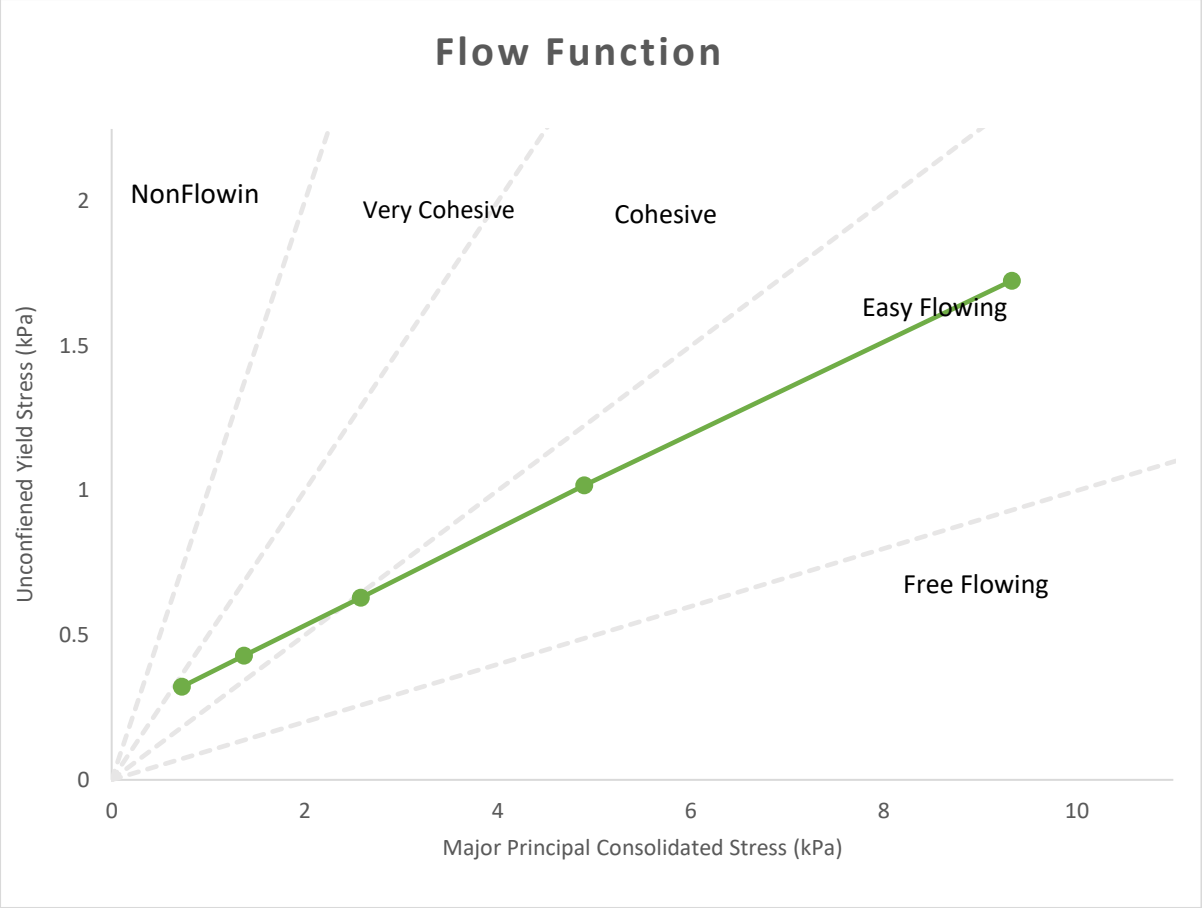

Fig 3.5: Flow function of Avicel PH 101

3.5.2 Wall friction and bulk density tests

These tests have been conducted by using 5-inch wall friction lid (SS – 304 stainless steel) which has 2B surface finish. The experimental procedure for these tests remains similar to flow function test barring change of lid to the flat lid 5-inch PFT – 516 is used and the flat profile is generated on the perforated trough. The yield locus is generated at the maximum load of 4.819 kPa, 1 displacement level is measured with an even spacing of 6 mm and a total of 10 stress set-points are calculated.

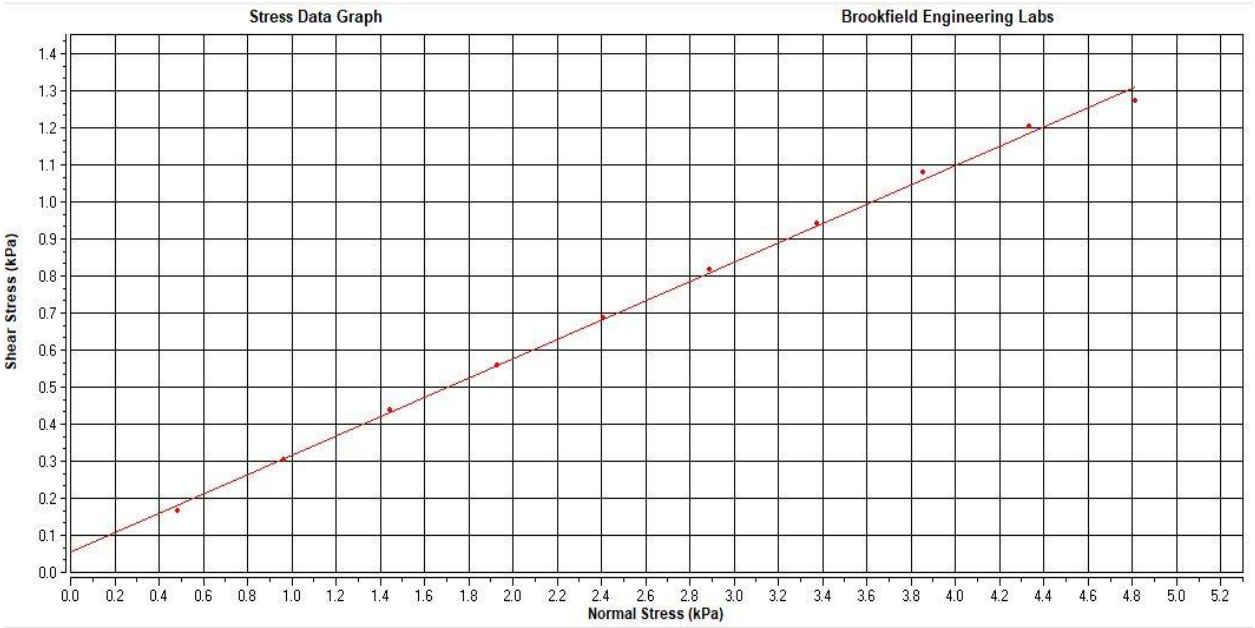

Fig 3.6: Yield locus for wall friction of Avicel PH 101

For the calculation of bulk density, peak stress applied on the powder is kept same at 4.819 kPa whereas the total number of stress set-points are 5.

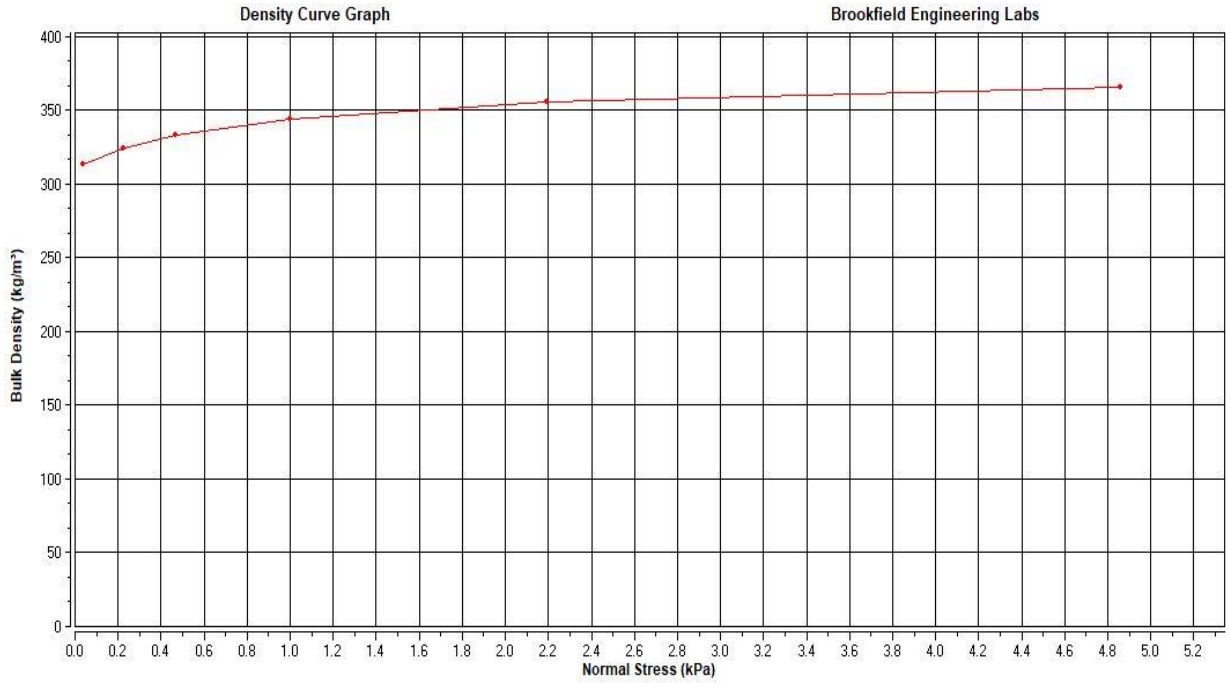

Fig 3.7: Bulk density variation of Avicel PH 101

3.6 Hopper designing for mass flow hopper

Hopper Half Angle (Θ) is a parameter used to identify the dimensions of the silo/hopper for a desired mass flow to occur. The mathematical relations for the designing of hoppers has been derived by Jenike (1964) and critical hopper dimensions have been made compared to the flow properties of the powder. These results have been explained in the form of charts in order to precisely find the dimension under which the powder will flow freely without a lot of intervention from the operator for non-flow of powders.

The formula for the calculation of hopper half angle comprises of inputs from both flow function test and wall friction test (Brookfield PFT). Depending on the design parameters angle found out comprises of all the 5-stress set-points measured previously.

For mass flor the governing equation for hopper half angle for conical hoppers is:

$$\Theta = \left[90 - \frac{1}{2}\, arccos\left(\frac{1-sin\delta j}{2\, cos\delta j}\right)\right] - \frac{1}{2}\left[\phi w + arcsin\left(\frac{sin\phi w}{sin\delta j}\right)\right] \quad (3.5)$$

where,

Θ = Hopper half angle (degree),

δ_j = Angle of internal friction (degree), and

ϕ_w = mass flow limit of angle of wall friction (degree)

3.7 Hand blending the excipients

In addition to the comparison of flow properties between pure Avicel PH 101 and Avicel PH 102, hand blended mixtures of 150 g each have been created with the addition of hydrophobic silica R972. According to the Food and Drug Administration (2009) the addition of guest particles cannot exceed 2 wt %. The blends are made by surface area coverage basis.

The formula of the calculation of surface area coverage is as follows (Yang et al., 2005):

$$Gwt\% = [(N\, d^3\, \rho\, d)/((D^3\, \rho_D)+(Nd^3\, \rho_d))] * 100 \quad (3.6)$$

$$N = 4\,(D+d)^2\,/d^2 \quad (3.7)$$

$$SAC\% = (wt\%\ of\ silica\ /\ Gwt\%) * 100 \quad (3.8)$$

$$Wt\ \%age\ of\ silica = SAC * Gwt\% / 100 \quad (3.9)$$

The blends are created by mixing 50 g of excipient with corresponding weight of silica and shaking it for 10 minutes. Repeating the process 2 more times and then mixing all of it together and then shaking it for another 5 minutes.

3.8 Tabletability

Tabletability is an important parameter in the context of drug powders. It is beneficial to understand the effect of flow enhancements over tabletability. Generally, as the flow of powders tend move on the free-flowing region, it becomes difficult for the powder to have a good tablet strength. As the size to the particle increases there is a reduction in tabletability (Sun et al., 2006).

The process that has been undertaken is as follows:

Tablets have been formed of two different weights, these are 100 mg and 200 mg (with tolerance of 10 wt%), these have been manufactured in the Pharmaceutical Branch, Chitkara University.

In addition to variation in weight of tablets, a total of three compaction forces have been applied in order to measure the change that is brought by increase in compaction force. These forces are 0.75, 1 and 1.25 Metric Ton. A total of 4 tablets of each SAC% have been formed. Then the tablets have been placed vertically, under a mechanical spring-loaded plunger to find the tablet strength of each tablet.

Chapter 4

Results and Discussions

Introduction

In this section, testing of results from the equipment described in the previous section have been discussed. The physical and flow properties difference between Avicel PH 101 and Avicel PH 102 have been discussed. Flow properties variation with the involvement of glidant R972 (as per SAC) with both the excipients has been discussed. And the effect of flow enhancements over the tabletability is compared.

4.1 Physical Properties

4.1.1 Bulk density test

Bulk density test when performed in the PFT provides the following result:

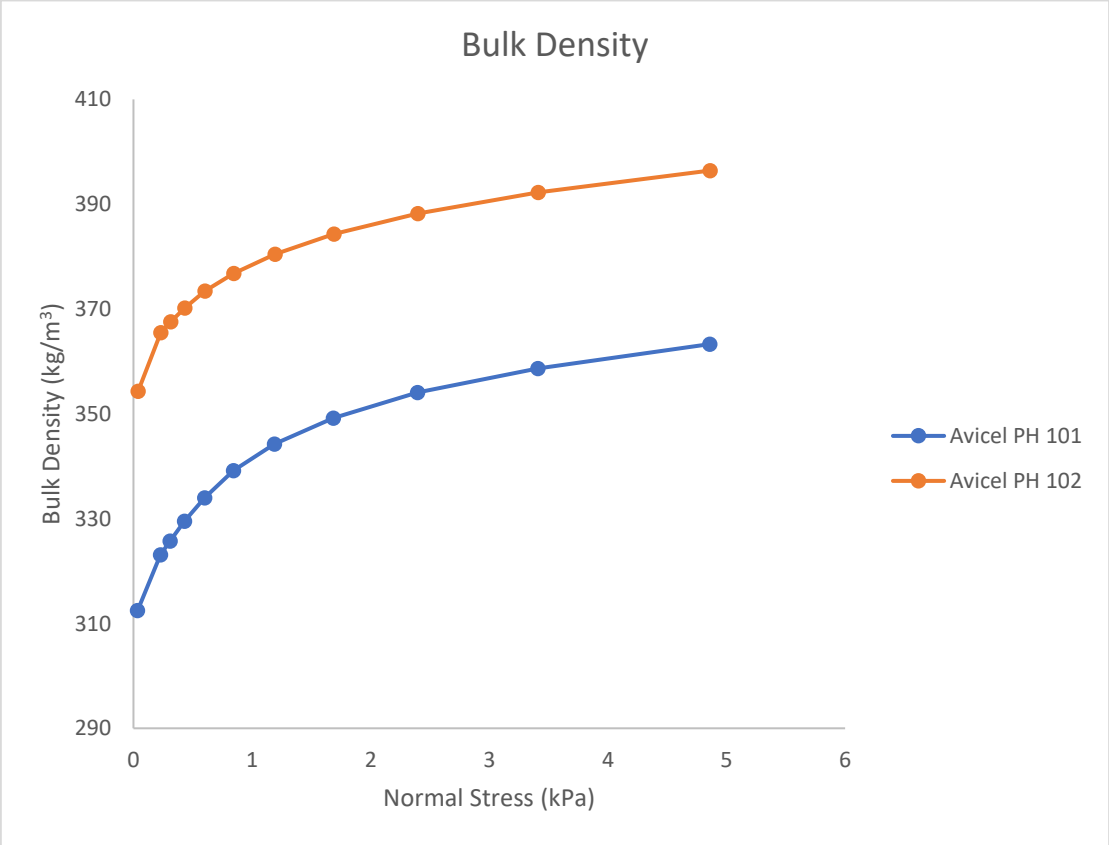

Fig 4.1: Bulk density curve comparison between Avicel PH 101 and Avicel PH 102 (AR)

The bulk density of Avicel PH 101 and Avicel PH 102 at the first stress point of 0.035 kPa and 0.042 kPa is 313.6 kg/m^3 and 383.3 kg/m^3 respectively and at the final stress point of 4.819 kPa is 353.2 kg/m^3 and 451.8 kg/m^3 respectively

The compressibility index of Avicel PH 101 obtained is 14.7 and of Avicel PH 102 is 15.16. Manually, the test conducted at zero (0) stress level has the average bulk density for Avicel PH 101 as 308.8 kg/m^3 and for Avicel PH 102 as 398.14 kg/m^3 which are collaborated by the machine readings.

4.1.2 Scanning Electron Microscopy (SEM)

Scanning electron microscopy (SEM) images are taken to understand the particle shape of the excipients and its effect on the flow properties. As shown in the Figure 4.2a and Figure 4.2b both the Avicel PH 101 and Avicel PH 102 corresponds to the particles shape being irregular/flaky, as the longer dimension of an average particle is 5 times longer the shorter dimension (Schulze, 2008). The particle shape is not spherical therefore, the packing fraction of the powder is less compared to similar diameter spherical particles.

Other key properties concurred with the irregular shape of the powder is the flow function. The powder tends to be more flowing as compared to similarly sized powders having spherical particles. On the other hand, wall friction is adversely affected through the flaky particles as it increases the horizontal force on the wall by increasing the effective angle of wall friction (Schulze, 2008).

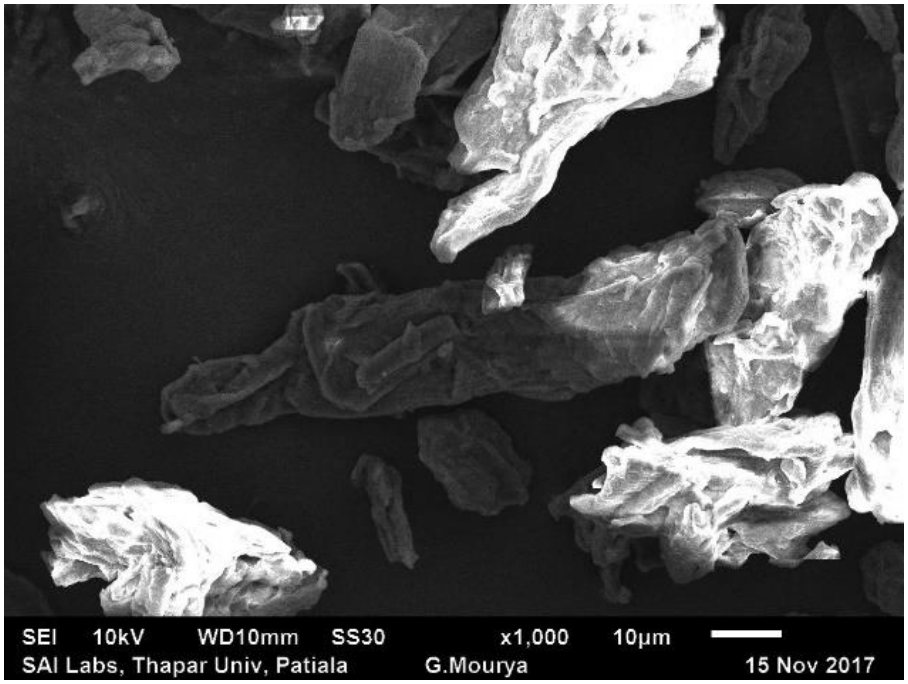

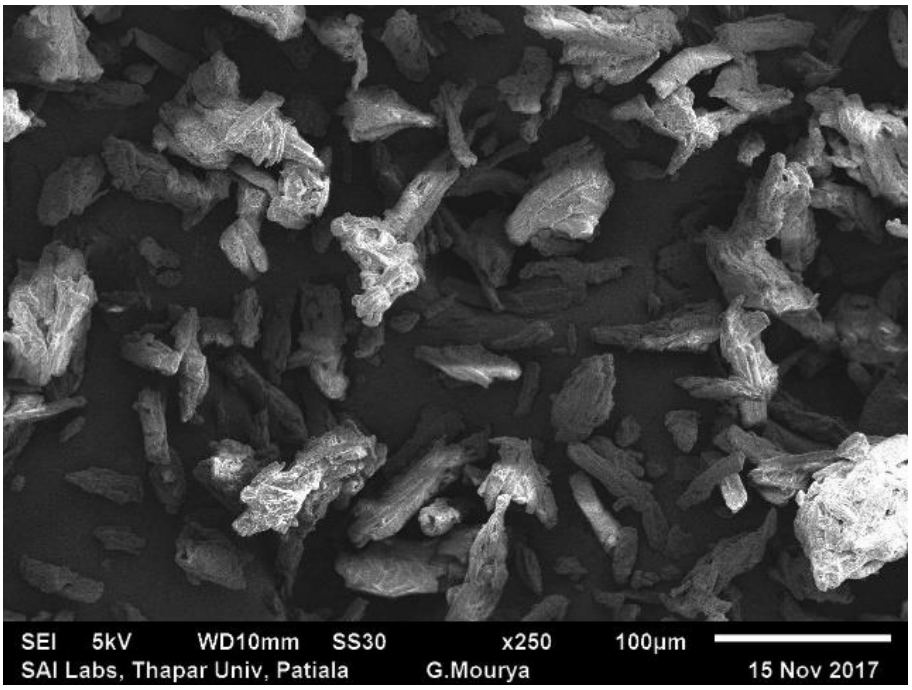

Fig 4.2a: SEM images of Avicel PH 101

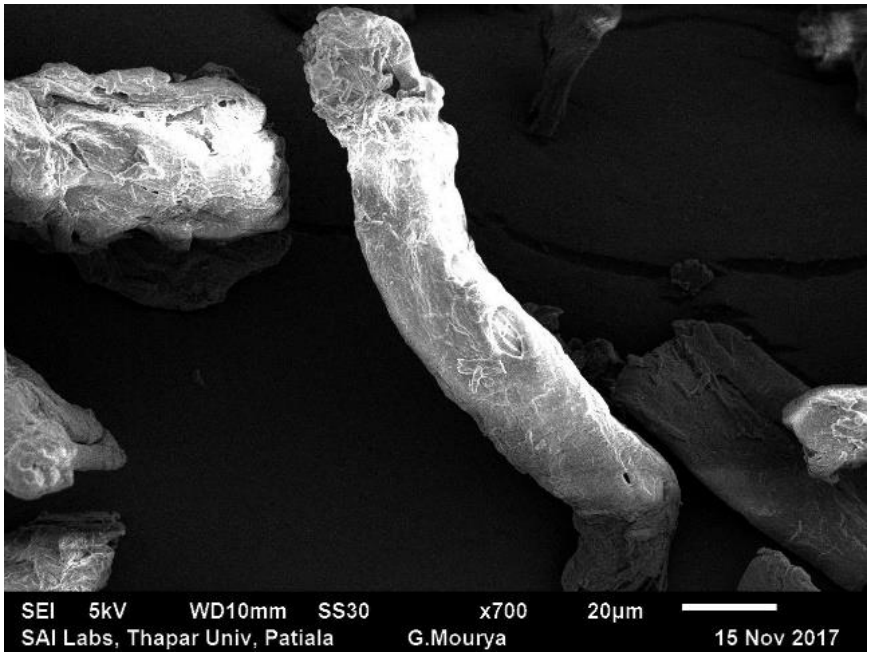

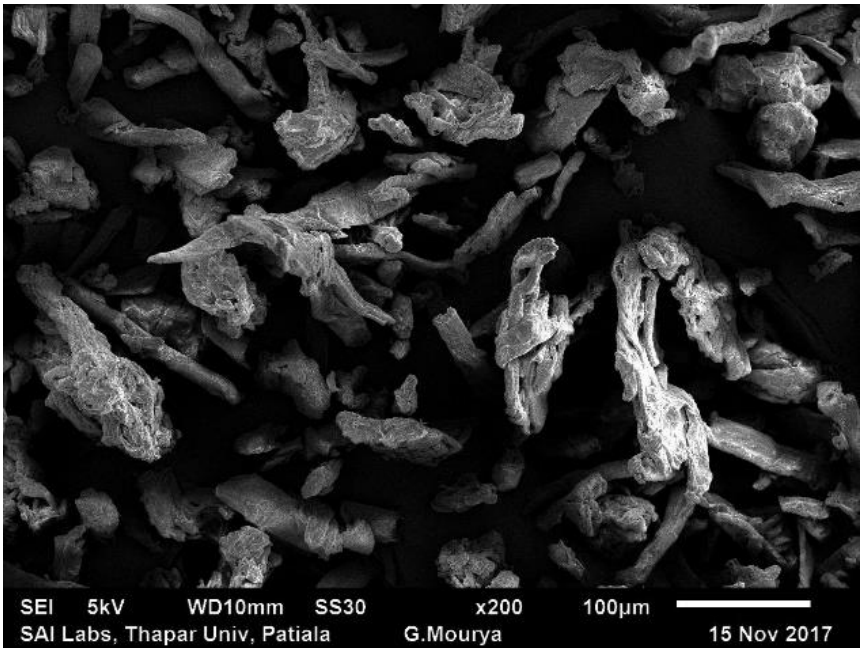

Fig 4.2b: SEM images of Avicel PH 102

4.1.3 Particle Size Distribution (PSD)

Particle size distribution test has been done to identify particle distribution and other parameters of the bulk solids. This test provides a detail description of the volume fraction of particle diameter present under a unit volume of bulk solid. The test has been conducted by using laser

diffraction method and the instrument used for the measurement is Mastersizer 2000. The measurements identified are d_{10}, d_{50}, $d_{90,}$ and span. These are shown in the Table 4.1.

Table 4.1: Physical properties of Avicel PH 101 and Avicel PH 102

Powders	d_{10} (μm)	d_{50} (μm)	d_{90} (μm)	ρ_p (kg/m^3)	ρ_b (kg/m^3)	ρ_t (kg/m^3)	HR	CI	Porosity	Span
Avicel PH 101	21.89	62.153	129.85	1525	308.8	389.27	1.26	14.7	0.797	1.737
Avicel PH 102	34.05	127.67	267.58	1130	398.14	488.27	1.22	15.16	0.647	1.829

The above measurements signify that Avicel PH 101 has d_{50} particle size 48% of Avicel PH 102. Comparing the Hausner Ratio of the two compounds shows that Avicel PH 101 belongs to category passable flow character and Avicel PH 102 belongs to fair flow character according to Uttia et al. (2014). Compressibility index (CI) of both Avicel PH 101 and Avicel PH 102 are comparable which implies at these powders show significant compression before consolidation and they show good tabletability property.

4.2 Flow properties comparison of Avicel PH 101 and Avicel PH 102

In this section, flow properties of both microcrystalline cellulose (MCC) Avicel PH 101 and Avicel PH 102 is compared. The parameters compared are flow function and wall friction.

4.2.1 Flow function test

This test has been performed by choosing the standard conditions on the Powder Flow Pro application. The stress points over which the powder strength has been measured are 0.289 kPa, 0.584 kPa, 1.180 kPa, 2.385 kPa and 4.819 kPa. The test has been repeated 5 times in order to eliminate any testing errors.

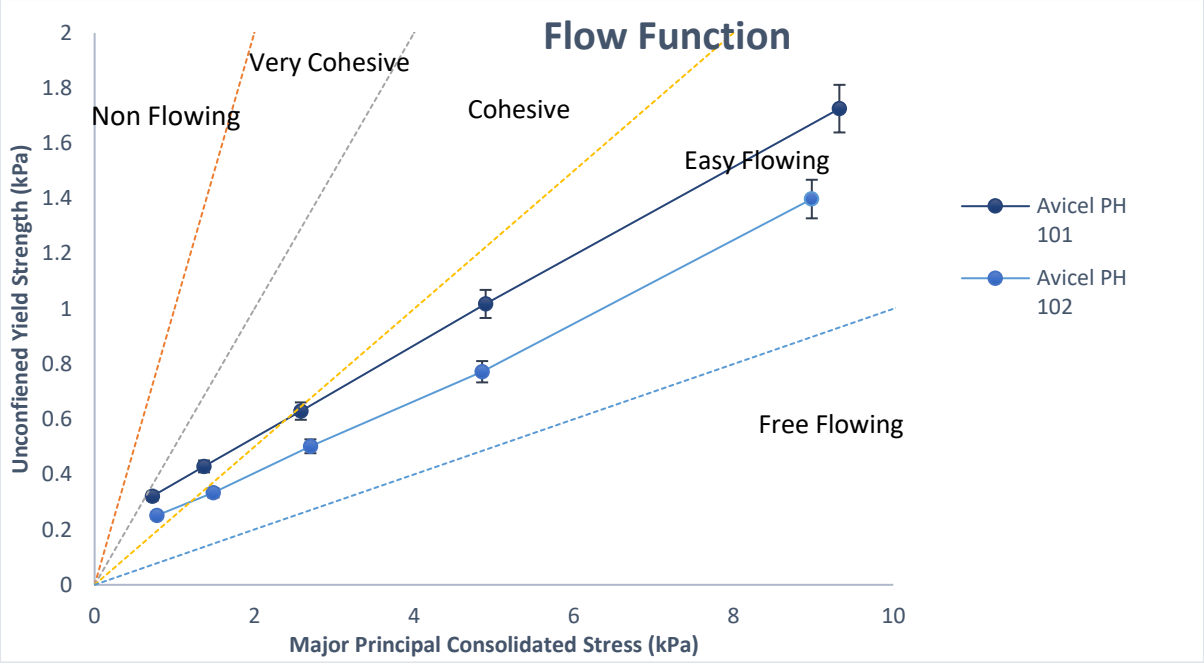

Fig 4.3: Flow function comparison Avicel PH 101 and Avicel PH 102 (AR)

Flow function property of both Avicel PH 101 and Avicel PH 102 lie in the easy flowing region. The flow Function (ff_c) of Avicel PH 101 comes out to be 5.4 whereas for Avicel PH 102 it is 6.42.

Avicel PH 102 has 18.88% more flowability as compared to Avicel PH 101. This is due to the low bulk density of Avicel PH 101 compared to Avicel PH 102 which implies that there is more air in same unit volume under no stress condition which provides more leeway for the Avicel PH 102 particles to flow. This has been validated with Faqih (2006) where standard deviation of flow index increases in the case of both Avicel PH 101 and Avicel PH 102. And flow index increases more in the case of Avicel PH 102.

4.2.2 Wall friction test

This test investigates the friction between the wall surface and the particles. The parameter calculated is the effective angle of wall friction, as it is an indicator of how much friction increases with increase in normal stress on a specific sample. Higher effective angle of wall friction indicates higher friction between the wall and the powder.

This test has been performed on a PFT by using standard quick wall friction test. A total of 10 stress set-points have been calculated which are divided in arithmetic progression. The graph depicting the comparison between the two powders has been shown below.

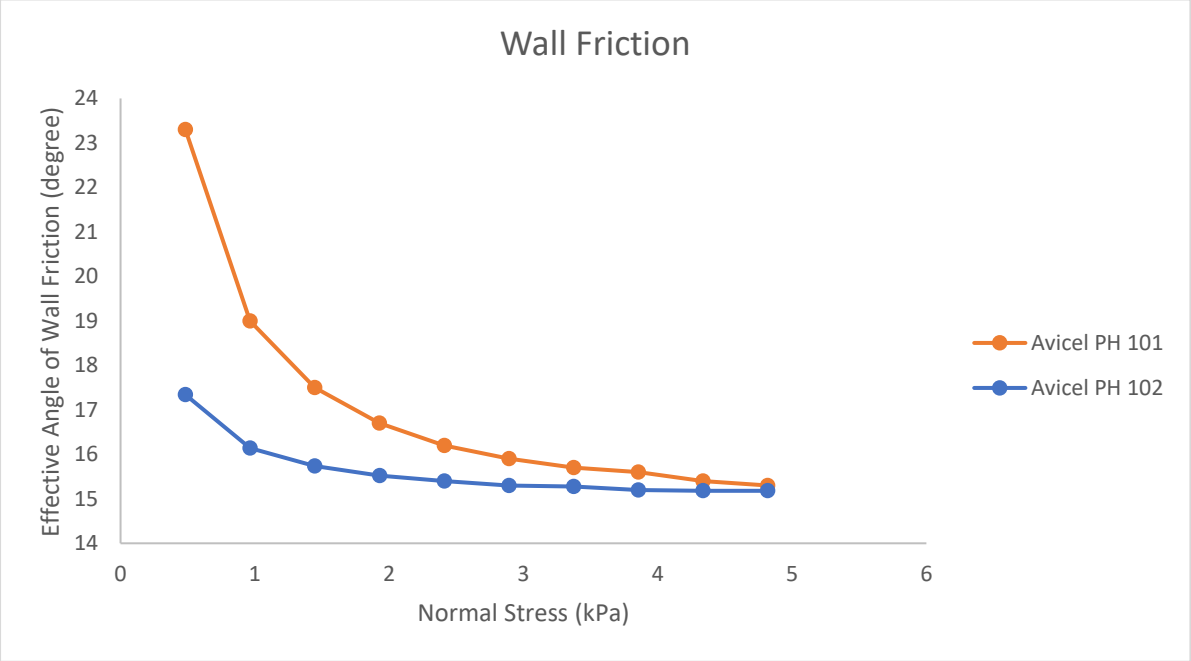

Fig 4.4: Wall friction comparison Avicel PH 101 and Avicel PH 102 (AR)

The observations made from the graph are as follows:

There is an inverse relationship between the effective angle of wall friction and normal stress applied on the powder.

The effective angle of wall friction of Avicel PH 101 is more than Avicel PH 102 and the change in wall friction angle with the normal stress happens more rapidly in case of Avicel PH 101 whereas the change in wall friction angle in case of Avicel PH 102 is gradual.

Avicel PH 102 has a 25.57 % advantage over Avicel PH 101 over the wall friction angle at the first stress point at 0.483 kPa. This stress advantage has been reduced to 0.007% at the last stress set-point at 4.817 kPa.

The validation of the above result can be asserted from Michrafy et al. (2003) where the effects of wall friction has been investigated in terms of relative density. The compounds compared are Avicel PH 101, Avicel PH 102 and Avicel PH 105. As concurred from the section 4.1.1, bulk density and normal stress has a constant trend in the researcher's investigation and shows a similar trend when the friction angle is varied with respect to bulk density.

4.3 Effect of flow enhancement over flow properties

As explained in an earlier section, blending the powder with glidants improves the powder flowability. The compound selected for the flow properties enhancements is hydrophobic silica R972. The limit of addition of any glidant in edibles is limited to 2 wt % as instructed in Food and Drug Administration (2009).

The surface area coverage of all the glidants is limited to 120%. The weight percentage at 120% SAC Avicel PH 101 is 0.332 wt % and for and for Avicel PH 102 is 0.224 wt % which is well under the limit of inclusion by the Food and Drug Administration (2009). Calculations for SAC and the weight of guest particles for 50 g gross weight of excipients is given below:

$$Gwt\% = [(N\, d^3\, \rho\, d)/((D^3\, \rho_D)+(Nd^3\, \rho_d))] * 100 \quad (4.1)$$

$$N = 4\,(D+d)^2\,/d^2 \quad (4.2)$$

$$SAC\% = (wt\%\ of\ silica\ /\ Gwt\%) * 100 \quad (4.3)$$

$$Wt\ \%age\ of\ silica = SAC * Gwt\% / 100 \quad (4.4)$$

Hydrophobic silica R972
Particle Diameter d_{32} = 20nm
Particle Density = 2650 kg/m^3

For Avicel PH 101
Particle Diameter d_{32} = 50 μm
Particle Density = 1525 kg/m^3

Gwt% = 0.27748 N = 25020004

Table 4.2: Silica addition in Avicel PH 101

SAC in %	20	40	60	80	100	120
%age wt of Silica	0.055496629	0.110993258	0.166489888	0.221986517	0.277483146	0.332979775
Corresponding to 50g	27.7mg	55.4mg	83.2mg	110.8mg	138.7mg	166.4mg

For Avicel PH 102

Particle Diameter d_{32} = 100 μm

Particle Density = 1130 kg/m^3

Gwt% = 0.187334 N = 100040004

Table 4.3: Silica addition in Avicel PH 102

SAC in %	20	40	60	80	100	120
%age wt of Silica	0.037466814	0.074933629	0.112400443	0.149867258	0.187334072	0.224800886
Corresponding to 50g	18.73mg	37.46mg	56.20mg	74.93mg	93.66mg	112.40mg

4.3.1 Bulk density variation by varying SAC

Bulk density is an extensive property that determines the flowability, compressibility and provides an idea of flow characteristics of the powder. This property has been measured below:

4.3.1.1 Variation in bulk density in Avicel PH 101

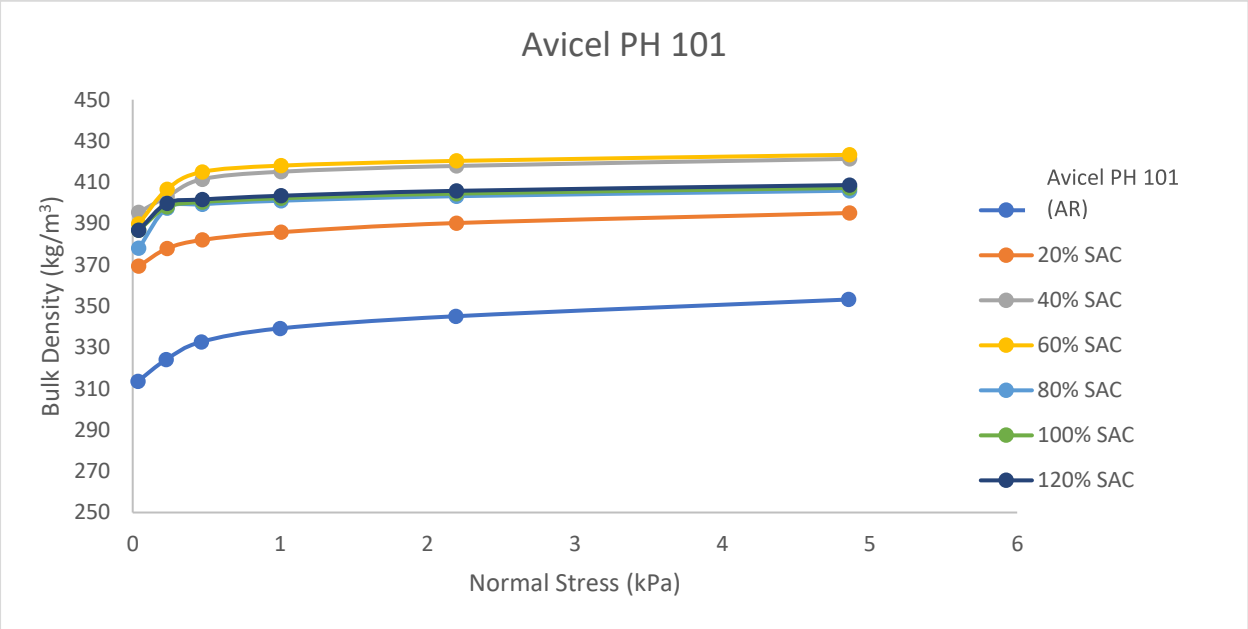

Fig 4.5: Variation in bulk density of Avicel PH 101 by varying silica SAC

Table 4.4: Variation in bulk density of Avicel PH 101 by varying SAC

Product	%age Change	Increase/Decrease
20% SAC over AR Avicel PH 101	11.86	Increase
40% SAC over 20% SAC	6.63	Increase
60% SAC over 40% SAC	0.474	Increase
80% SAC over 60% SAC	4.11	Decrease
100% SAC over 80% SAC	0.332	Decrease
120% SAC over 100% SAC	0.282	Decrease

There is a certain increase in bulk density with silica inclusion with respect to “as received” Avicel PH 101. The peak bulk density is observed for Avicel PH 101 at 60% SAC of silica and after this the bulk density decreases to 395 kg/m^3 in Avicel PH 101 with 120% SAC of silica.

4.3.1.2 Variation in bulk density in Avicel PH 102

In contrast to the behaviour of the samples in Avicel PH 101, we have observed that in Avicel PH 102, the addition of silica decreases the bulk density. The highest decrease in bulk density has been noticed when 20% SAC of silica is included which is 12.97% decrease compared to as received Avicel PH 102. But with further increase in silica, the bulk density increases gradually with only decrease noticed in the samples of Avicel PH 102 with 80% SAC silica.

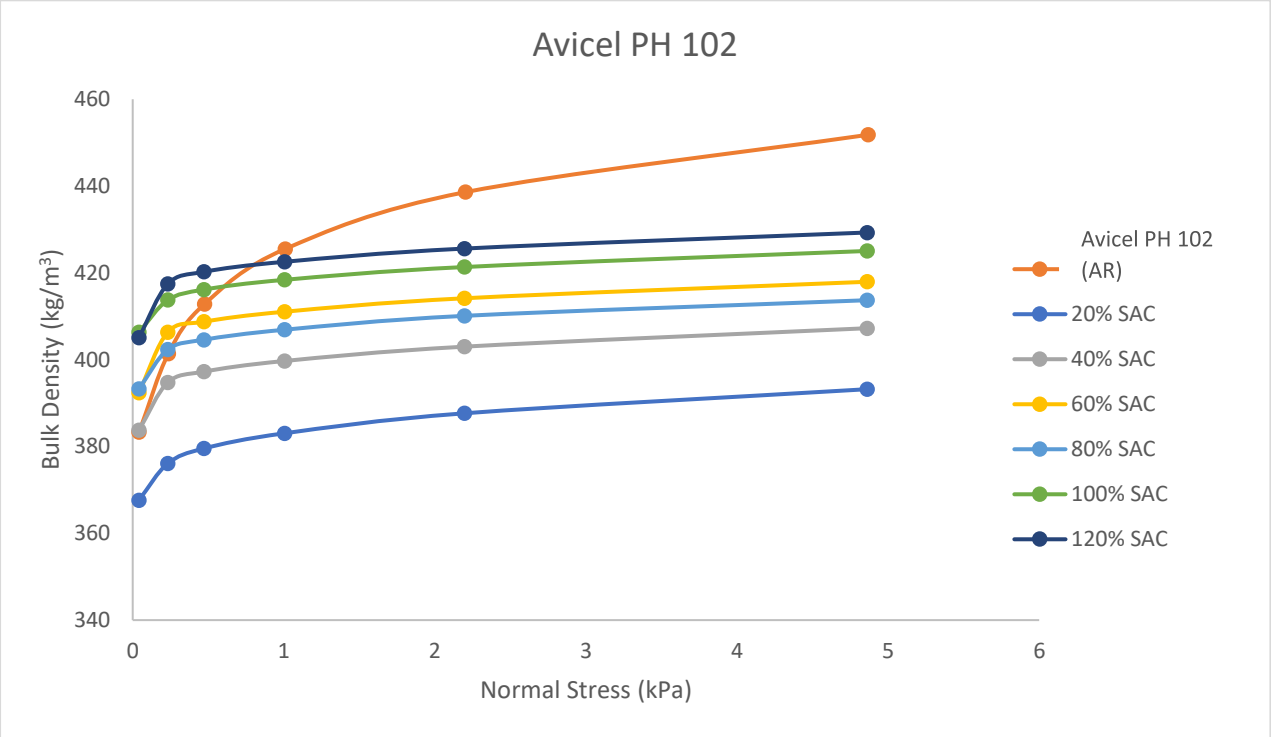

Fig 4.6: Variation in bulk density of Avicel PH 102 by varying silica SAC

Table 4.5: Variation in bulk density of Avicel PH 102 by varying silica SAC

Product	%age Change	Increase/Decrease
20% SAC over AR Avicel PH 102	12.97	Decrease
40% SAC over 20% SAC	3.56	Increase
60% SAC over 40% SAC	2.62	Increase
80% SAC over 60% SAC	1.01	Decrease
100% SAC over 80% SAC	2.74	Increase
120% SAC over 100% SAC	0.999	Increase

4.3.2 Flow function comparison by varying SAC

4.3.2.1 Flow function test of Avicel PH 101

The prerequisites of the testing is the same as earlier flow function test, these tests have been performed by choosing the standard conditions on the Powder Flow Pro application. The stress points over which the powder strength has been measured are 0.289 kPa, 0.584 kPa, 1.180 kPa, 2.385 kPa and 4.819 kPa. The test has been repeated 5 times in order to eliminate any testing errors.

The observations from the experiments comparison are:

With increase in silica SAC, the unconfined yield strength of the particles decreases. The increase in flowability of 20% SAC sample over "as received" Avicel PH 101 is 31.52%. Similarly, 40% SAC sample has 26.81% increase compared to 20% SAC sample, 60% SAC sample has 25.99% increase compared to 40% SAC sample, 80% SAC sample has 41.4% increase compared to 60% SAC sample, but 100% SAC sample has only 2.51% increase compared to 80% SAC sample and 120% SAC sample has 4.55% increase compared to 100% SAC sample.

Slippage between layers takes place when 0.584 kPa, 1.180 kPa and 2.385 kPa consolidating stresses are applied to samples having high nano silica content. This is because, as more surface of Avicel PH 101 is covered with silica particles, surface – surface adhesion between individual particles reduces and individual particles of Avicel PH 101 are able to move more freely.

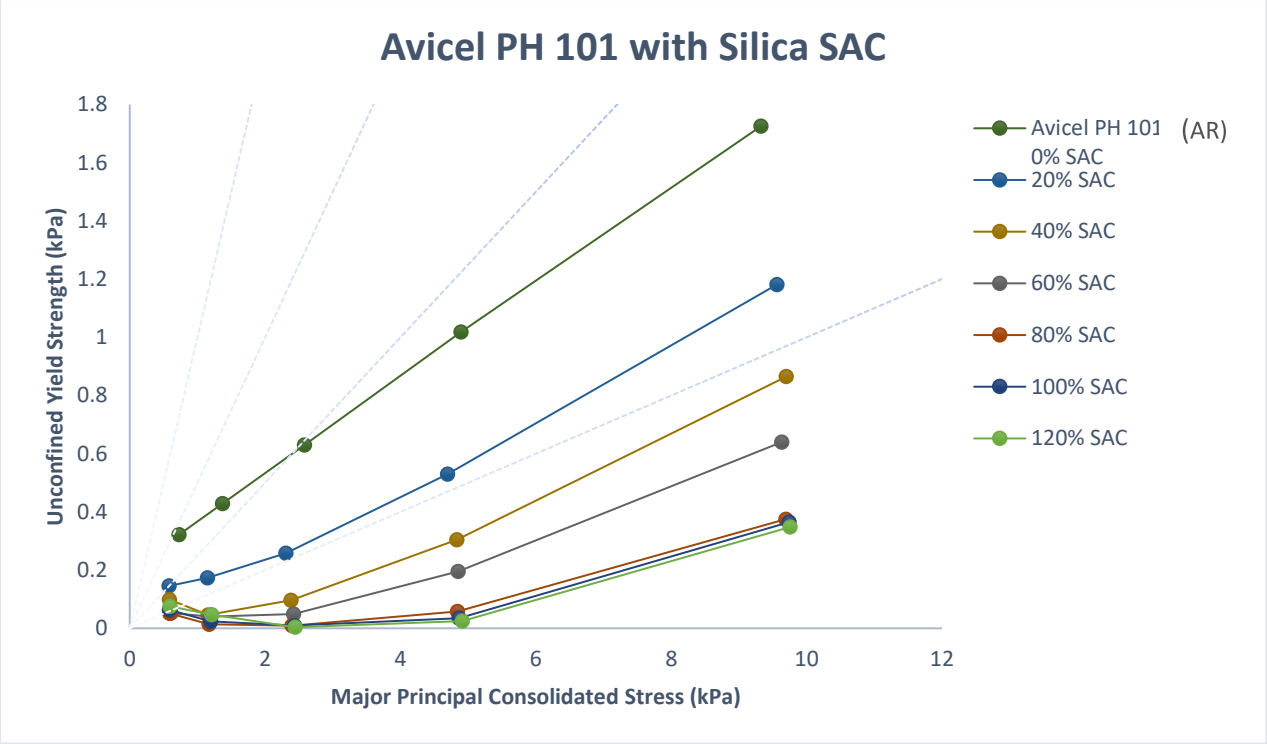

Fig 4.7: Flow function comparison of Avicel PH 101 by varying silica SAC

4.3.2.2 Flow function test of Avicel PH 102

The prerequisite of the testing is the same as earlier flow function test, these tests have been performed by choosing the standard conditions on the Powder Flow Pro application. The stress points over which the powder strength has been measured are 0.289 kPa, 0.584 kPa, 1.180 kPa, 2.385 kPa and 4.819 kPa. The test has been repeated 5 times in order to eliminate any testing errors.

The observations from the experiments comparison are:

Unlike Avicel PH 101 where the increase in flowability is 31.52% for 20% SAC silica over as received Avicel PH 101, improvement in flowability in Avicel PH 102 with increase in silica is gradual.

With increase in silica SAC, the unconfined yield strength of the particles decreases. The increase in flowability of 20% SAC sample over as received Avicel PH 102 is 9.02%. Similarly, 40% SAC sample has 8.69% increase compared to 20% SAC sample, 60% SAC sample has 10.88% increase compared to 40% SAC sample, 80% SAC sample has 12.78% increase compared to 60% SAC sample, 100% SAC sample has only 12.42% increase

compared to 80% SAC sample and 120% SAC sample has 12.42% increase compared to 100% SAC sample.

Slippage between layers takes place when 0.584 kPa, 1.180 kPa and 2.385 kPa consolidating stresses are applied to samples having high nano silica content. This is because, as more surface of Avicel PH 102 is covered with silica particles, surface – surface adhesion between individual particles reduces and individual particles of Avicel PH 102 are able to move more freely.

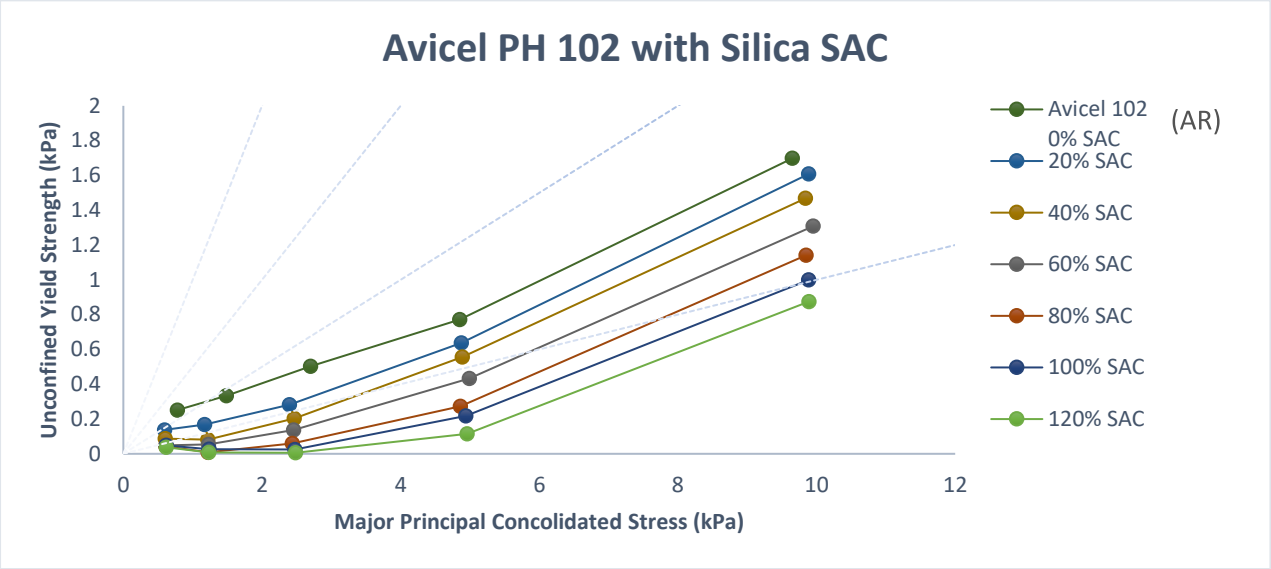

Fig 4.8: Flow function comparison of Avicel PH 102 by varying silica SAC

With the increase in silica SAC, flow function increases. There is a gradual increase in flow function and 120% SAC Avicel PH 102 has a flow function of 11.3. But this flow function is less than Avicel PH 101 120% SAC sample which has 28.03 flow function.

It is due to the addition of silica R972, surface area contact reduces that in turn requires the particles less force to flow. This is more significant at lower silica inclusions of Avicel PH 101 samples while in Avicel PH 102 samples there is a gradual rise in flow function with silica addition.

The validation of the above two sections has been done by Faqih (2006) and Wang et al. (2016) where flow functions of both Avicel PH 101 and Avicel PH 102 are calculated. It has been identified that with the increase in glidant inclusion, flowability of the sample increases.

4.3.3 Wall friction comparison by varying SAC

4.3.3.1 Wall friction test of Avicel PH 101

This test investigates the friction between the particles and the wall surface. The parameter calculated is the effective angle of wall friction as it is an indicator of the how much friction increases with increase in normal stress. Higher wall friction angle indicates higher friction between the wall and the powder.

This test has been performed on a PFT by using the option “standard quick wall friction test”. A total of 10 stress set-points have been calculated which are divided in an arithmetic progression. The graph depicting the comparison between the two powders has been shown below.

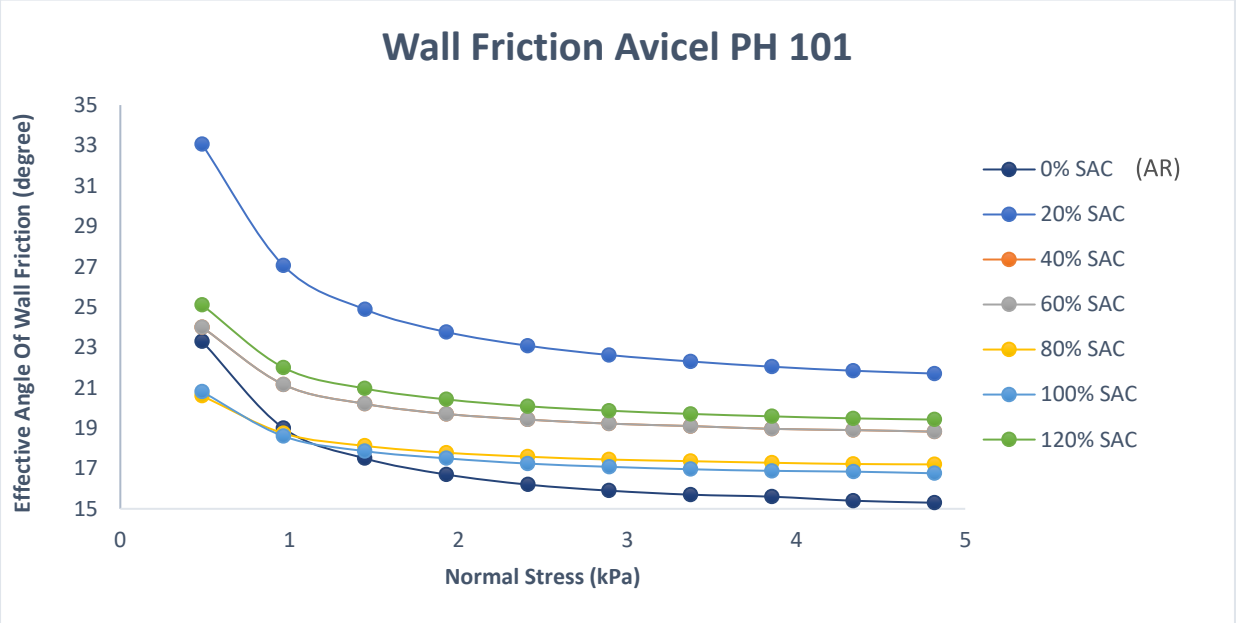

Fig 4.9: Wall friction comparison of Avicel PH 101 with varying silica SAC

The observations from the experiments comparison are:
As the flow function of the sample increases with increase in silica content which helps the flowability of the powder moving down the hopper which lowers the surface – surface interactions of the samples. Wall friction angle also shows an increase which hinders the flow of powder, as the powder pushes towards the hopper wall and potentially gets consolidated creating a funnel flow situation.

The wall friction angle of “as received” Avicel PH 101 has the least friction angle. With increase in silica, certainly wall friction angle increases in Avicel PH 101 particles but there is no certain trend.

This is due to the irregular/flaky shape of the particles which adheres more with the wall as compared to spherical shaped particles.

Table 4.6 Wall friction comparison of Avicel PH 102 by varying silica SAC

Product	%age Change	Increase/Decrease
20% SAC over AR Avicel PH 101	41.83	Increase
40% SAC over 20% SAC	13.27	Decrease
60% SAC over 40% SAC	0.32	Decrease
80% SAC over 60% SAC	5.31	Decrease
100% SAC over 80% SAC	2.5	Decrease
120% SAC over 100% SAC	13.69	Increase

4.3.3.2 Wall friction test of Avicel PH 102

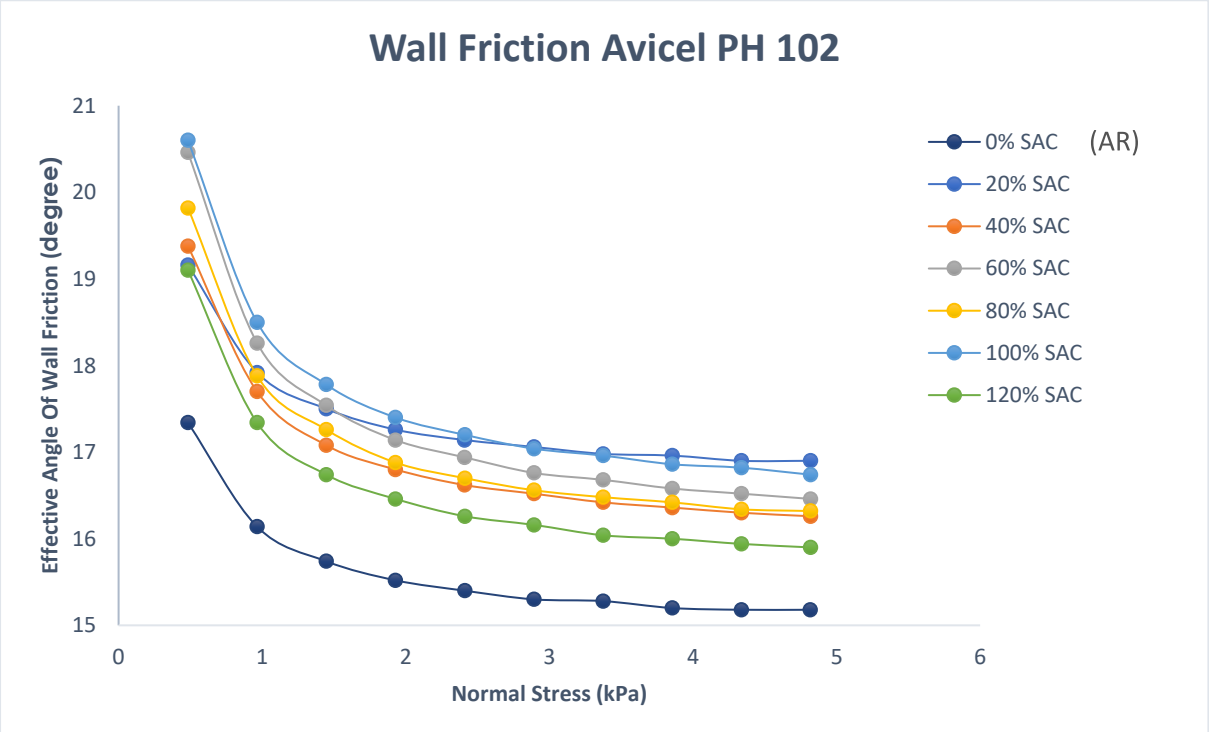

Fig 4.10: Wall friction comparison of Avicel PH 102 by varying silica SAC

The observations from the experiments comparison are:
As the flow function of the sample increases with increase in silica content which helps the flowability of the particles moving down the hopper which lowers the surface – surface interactions of the samples. Wall friction angle also shows an increase which on the other hand hinders the flow of powder, as the powder pushes towards the hopper walls and potentially gets consolidated creating a funnel flow situation.

The wall friction angle of "as received" Avicel PH 102 has the least friction angle. With increase in silica certainly wall friction angle increases in Avicel PH 102 particles but there is no certain trend.

This is due to the irregular/flaky shape of the particles which adheres more with the wall as compared to spherical shaped particles.

Table 4.7: Wall friction comparison of Avicel PH 102 by varying silica SAC

Product	Percentage Change	Increase/Decrease
20% SAC over AR Avicel PH 102	11.33	Increase
40% SAC over 20% SAC	3.78	Decrease
60% SAC over 40% SAC	1.23	Increase
80% SAC over 60% SAC	0.85	Decrease
100% SAC over 80% SAC	2.57	Increase
120% SAC over 100% SAC	5.01	Decrease

4.3.4 Hopper half angle for mass flow by varying SAC

With the discussion in the above sections, we know that as the glidant enhances the flowability of the samples which benefits the flow. Whereas the wall friction also increases which hinders the flow. To obtain a complete picture of the particle flow, hopper half angle of the samples have been calculated which is required to the known in a practical situation.

For mass flow the governing equation for hopper half angle for conical hoppers is:

$$\Theta = \left[90 - \frac{1}{2}\, arccos\left(\frac{1-sin\delta j}{2\, cos\delta j}\right)\right] - \frac{1}{2}\left[\phi w + arcsin\left(\frac{sin\phi w}{sin\delta j}\right)\right] \quad (4.5)$$

Where,

Θ = hopper half angle (degree),

δ_j = angle of internal friction(degree), and

ϕ_w = mass flow limit of angle of wall friction (degree)

For uniformity all hopper half angle measurements have been taken over 15 cm diameter opening.

4.3.4.1 Variation in hopper half angle in Avicel PH 101 with R972

Hopper half angle shows an increase with increase in silica SAC.

Table 4.8: Hopper half angle of Avicel PH 101 by varying silica SAC

Name	Hopper half angle
Avicel PH 101	28.3
With 20% SAC	28.4
With 40% SAC	28.6
With 60% SAC	29.4
With 80% SAC	30.4
With 100% SAC	31.9
With 120% SAC	33.7

When silica SAC is low, the percentage increase in hopper half angle is around ~0.705%, but with the increase silica content the change in hopper half angle is ~5.64% compared to the “as received Avicel PH 101.

This has been attributed to the large flow function increase as compared to wall friction angle change.

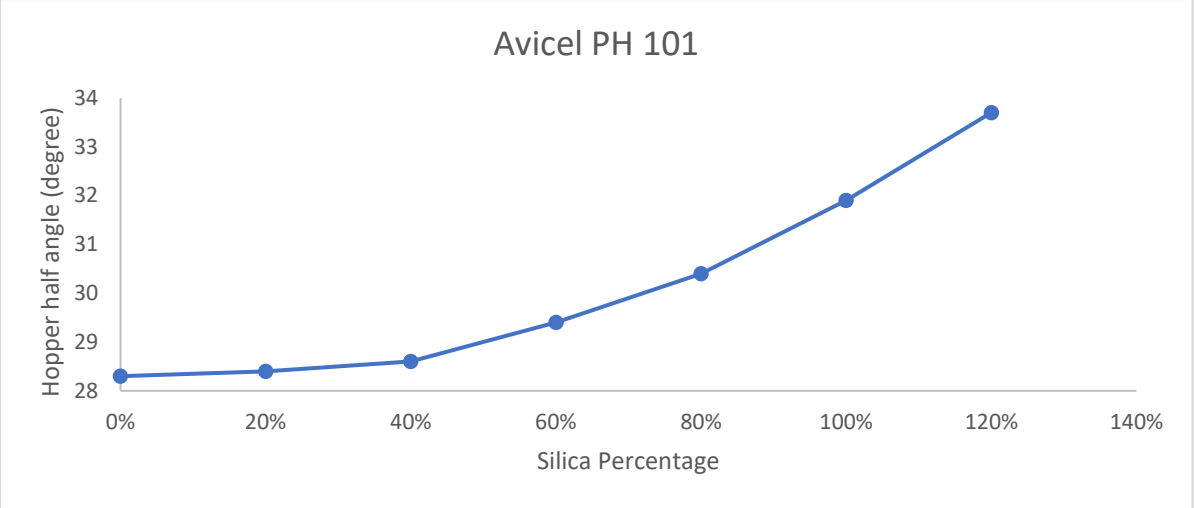

Fig 4.11: Variation in hopper half angle in Avicel PH 101 by varying silica SAC

4.3.4.2 Variation in hopper half angle in Avicel PH 102 with R972

Similar to Avicel PH 101, hopper half angles in silica blended Avicel PH 102 shows an increase.

Table 4.9: Hopper half angle of Avicel PH 102 by varying silica SAC

Name	Hopper half angle
Avicel PH 102	28.9
With 20% SAC	30.6
With 40% SAC	32.5
With 60% SAC	32.8
With 80% SAC	32.9
With 100% SAC	33.3
With 120% SAC	33.8

In contrast to Avicel PH 101, the silica inclusions with Avicel PH 102 that has high percentage change in the hopper half angle is observed when silica inclusion is low around, ~6.9%. At higher silica inclusions the percentage change increase in hopper half angle is ~1.7% compared to the Avicel PH 102 with 40% silica SAC.

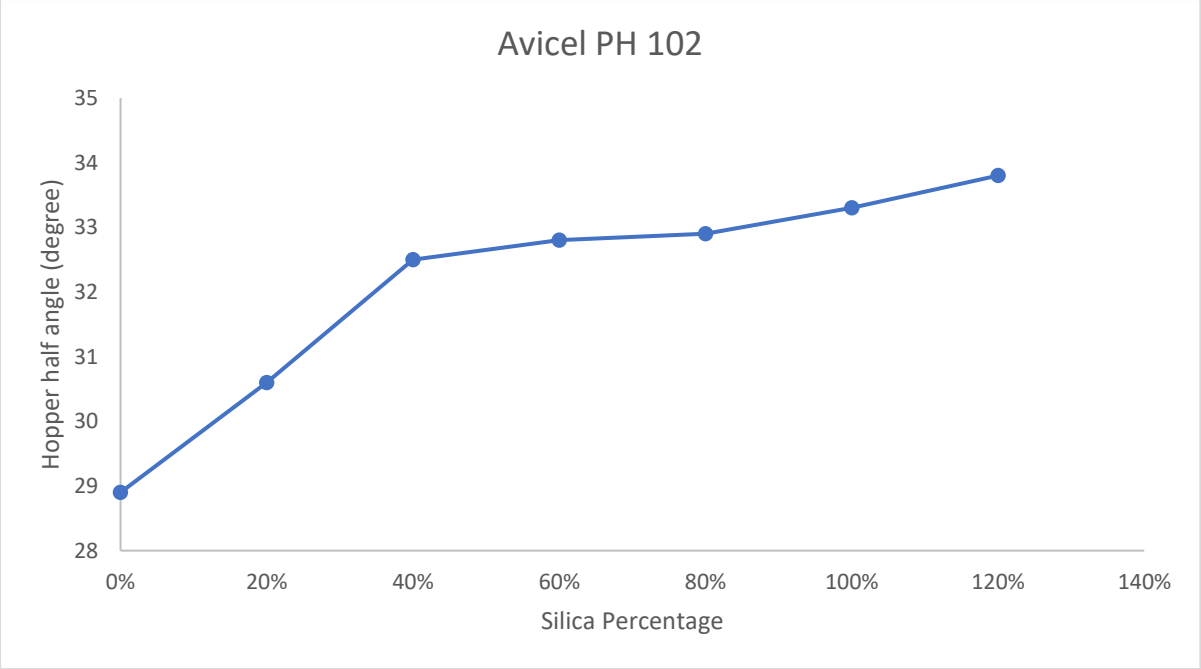

Fig 4.12: Variation in hopper half angle in Avicel PH 102 by varying silica SAC

This is due to high flowability with increase in silica SAC. As silica content increases, the flowability increases and the powder is more likely to flow at a higher hopper half angle.

This result can be validated by Faqih (2016) where hopper characteristics of Avicel PH 101 and Avicel PH 102 with addition of magnesium stearate as lubricant have been discussed with addition up to 2 wt % of the primary powder. The inclusion shows increase in the mass flow capability of the blends having more magnesium stearate. With increase in the addition of magnesium stearate, mass flow takes place at a lower slope.

4.3.5 Effect on cohesion and angle of internal friction

Cohesion and angle of internal friction are two properties that are also calculated through the Mohr circle calculations during the flow function test. Cohesion is the shear stress in the powder available when the normal stress applied on the sample is zero (0).

Whereas angle of internal friction is the friction angle made from the origin to the tangent on the consolidating yield strength.

Following are the readings for cohesion and angle of internal friction in all the Avicel PH 101 samples.

Table 4.10: Failure stress in Avicel PH 101 by varying silica SAC

Name	Principal Consolidated Stress (kPa)	Unconfined Yield Strength (kPa)	Angle of Internal Friction (degree)	Cohesion (kPa)
Avicel PH 101 with 0% SAC	0.7258	0.3216	44.6	0.073
	1.37	0.429	41.6	0.1005
	2.582	0.6296	40.7	0.154
	4.8958	1.0178	40.2	0.254
	9.3268	1.7256	40.3	0.457
Avicel PH 101 with 20% SAC	0.5824	0.1456	41.76	0.0376
	1.149	0.1734	39.82	0.0442
	2.3074	0.258	39.28	0.0648
	4.695	0.5294	39.42	0.1326
	9.5634	1.1816	39.74	0.296
Avicel PH 101 with 40% SAC	0.5862	0.098	40.46	0.0252
	1.1582	0.0462	38.74	0.0114
	2.3804	0.0962	39.2	0.0232
	4.8316	0.304	39.44	0.0742
	9.6988	0.8648	39.72	0.2128
Avicel PH 101 with 60% SAC	0.6094	0.0518	40.22	0.013
	1.1948	0.04	39.94	0.0096
	2.42	0.0494	39.48	0.012
	4.8536	0.1954	39.44	0.047
	9.6334	0.64	39.74	0.1554
Avicel PH 101 with 80% SAC	0.5882	0.0512	39.66	0.0128
	1.1732	0.0138	38.72	0.0032
	2.3972	0.009	38.8	0.0022
	4.8428	0.0578	39.1	0.014
	9.6924	0.375	39.3	0.0904
Avicel PH 101 with 100% SAC	0.5874	0.0638	40.68	0.0152
	1.1968	0.0238	39.68	0.0048
	2.4352	0.0096	39.3	0.0022
	4.866	0.0348	39.1	0.0082
	9.7406	0.3646	39.68	0.0872
Avicel PH 101 with 120% SAC	0.593	0.0754	41.26	0.0184
	1.2104	0.047	40.1	0.0112
	2.4456	0.0038	39.48	0.001
	4.9142	0.0248	39.3	0.006
	9.7556	0.348	39.6	0.0834

Following are the readings for cohesion and angle of internal friction in all the Avicel PH 102 samples.

Table 4.11: Failure stress in Avicel PH 102 by varying silica SAC

Name	Principal Consolidated Stress (kPa)	Unconfined Yield Strength (kPa)	Angle of Internal Friction (degree)	Cohesion (kPa)
Avicel PH 102 with 0% SAC	0.778	0.2512	42.86667	0.058
	1.4872	0.3334	40.26667	0.072333
	2.702	0.502	39.4	0.111
	4.8526	0.7722	38.9	0.185
	9.65	1.698	38.86667	0.441667
Avicel PH 102 with 20% SAC	0.595	0.1376	41.76	0.0338
	1.1714	0.1674	40.02	0.0422
	2.3956	0.2816	40.06	0.0698
	4.8742	0.6372	40.34	0.158
	9.8834	1.6078	41.04	0.4332
Avicel PH 102 with 40% SAC	0.6046	0.0876	41.1	0.0216
	1.2166	0.0814	40.1	0.0198
	2.4634	0.203	40.18	0.0494
	4.8914	0.5568	40.36	0.1368
	9.8392	1.468	40.92	0.3652
Avicel PH 102 with 60% SAC	0.6166	0.0486	40.28	0.0116
	1.229	0.0544	39.84	0.013
	2.4574	0.1374	39.72	0.033
	4.9908	0.4336	39.56	0.1086
	9.9518	1.3082	40.88	0.3212
Avicel PH 102 with 80% SAC	0.613	0.0434	40.46	0.0106
	1.222	0.0086	39.62	0.002
	2.4354	0.0598	39.58	0.0142
	4.8626	0.272	39.86	0.0654
	9.8476	1.141	40.74	0.2784
Avicel PH 102 with 100% SAC	0.6172	0.0476	40.4	0.0112
	1.2348	0.0258	39.92	0.006
	2.4762	0.0248	39.56	0.006
	4.9396	0.2172	39.84	0.052
	9.8876	0.9992	40.52	0.243
Avicel PH 102 with 120% SAC	0.6172	0.037	40.48	0.009
	1.2326	0.0074	39.82	0.0018
	2.4816	0.0058	39.62	0.0012
	4.9592	0.1148	39.92	0.0272
	9.891	0.875	40.46	0.214

4.3.5.1 Effect on cohesion by varying SAC

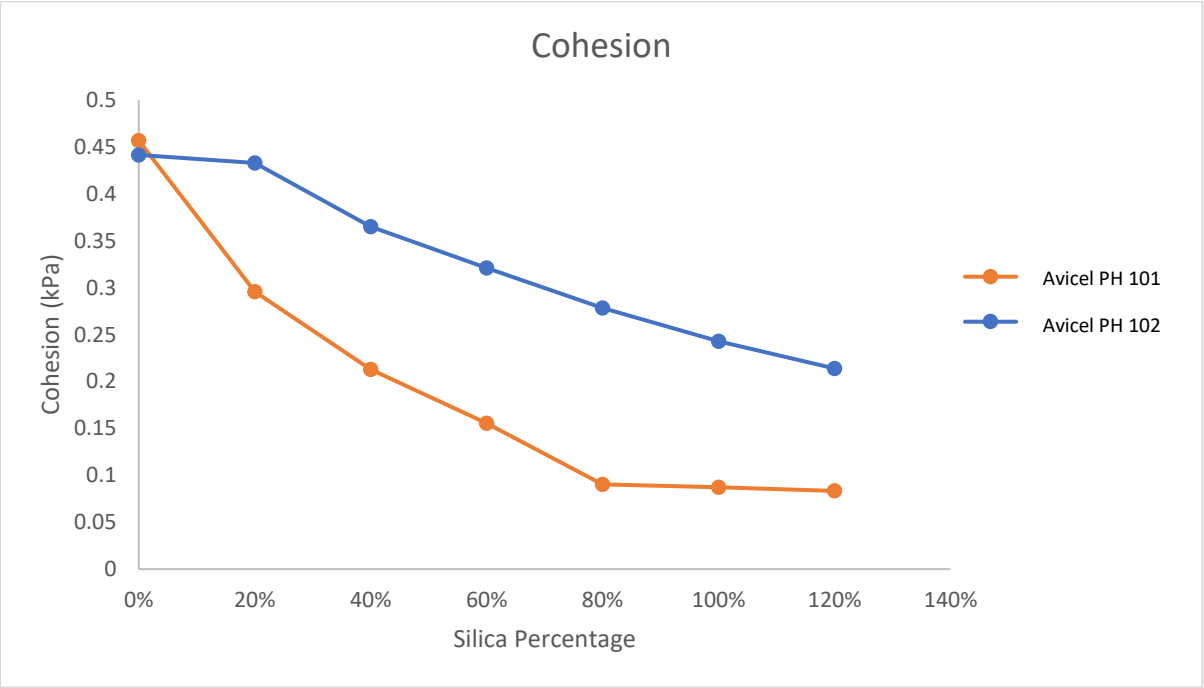

Fig 4.13: Change in cohesion of Avicel PH 101 and Avicel PH 102 by varying silica SAC

The observations from the cohesion values are:

There is a decrease in cohesion strength in the powder with increase in silica SAC.

The effect of silica SAC over cohesion is less in Avicel PH 102 samples with total variation (δ) of 0.227 kPa or percentage change of 51.47%. Whereas the effect of silica SAC over cohesion strength is more in Avicel PH 101 samples with total variation (δ) of 0.451 kPa or a reduction of 98.68%.

The variation in the cohesion values in Avicel PH 102 are gradual and linear whereas in Avicel PH 101 samples, the variation is asymptotic with the variation in cohesion from 100% SAC to 120% SAC being only 0.002 kPa.

4.3.5.2 Effect on angle of internal friction by varying SAC

The observations from the Angle of internal friction values are:

Same as cohesion, angle of internal friction also decreases with increase in silica content. The span of variation of angle of internal friction with increase in silica SAC in Avicel PH 101 is

5.3° or 11.88%. Similarly, in Avicel PH 102 samples, the variation on the angle of internal friction is only 2.4° or 5.56%.

The variation in the angle of internal friction in Avicel PH 101 samples shows an asymptotic path with peak internal friction angle being 44.6° and the minimum of 39.3° whereas in the Avicel PH 102 there is a sudden decrease in internal friction angle from “as received” Avicel PH 102 sample to 20% SAC sample and the variation is 1.82° or 4.24%. The total variation from 20% SAC silica inclusion to 120% SAC silica inclusion the total variation is 0.56° or 1.4%.

These cohesion and angle of internal friction results are formed due to Mohr circle’s intercepts in the flow function test. The respective powders clearly show increase in flowability with increase in silica R972.

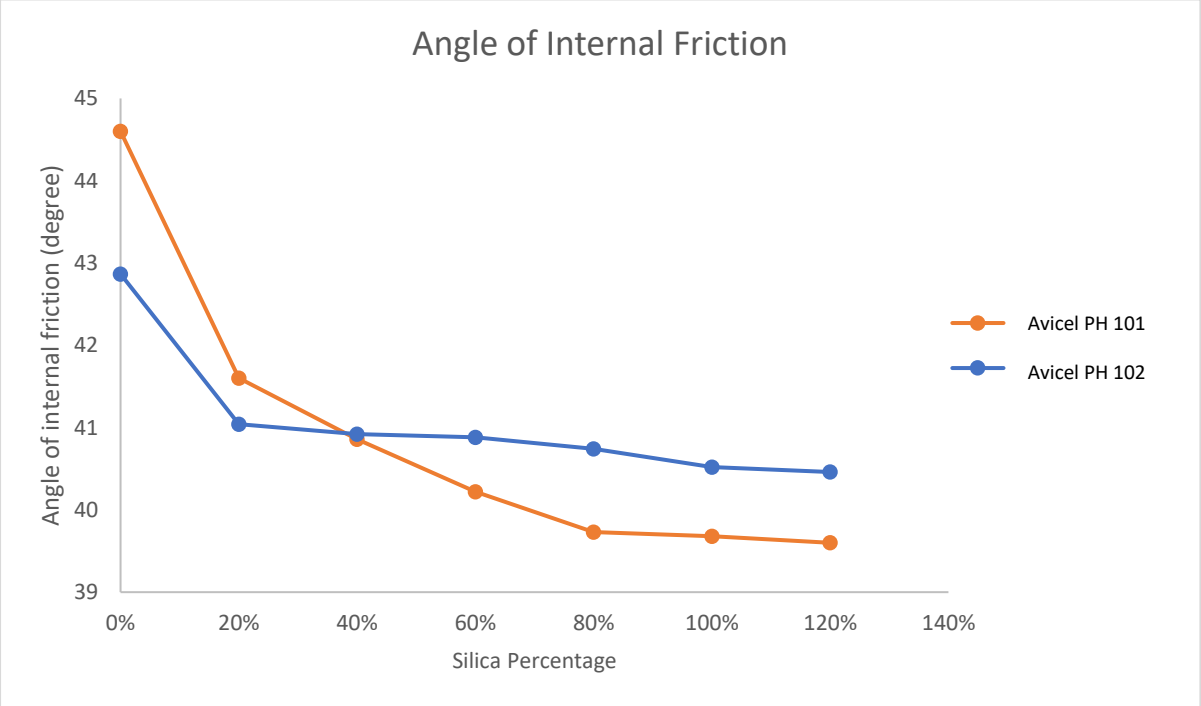

Fig 4.14: Change in internal friction of Avicel PH 101 and Avicel PH 102 by varying silica SAC

4.4 Effect on tabletability by varying SAC

This test is performed to ensure that the tablet will not break in the process of converting the powder into tablets, packaging and transportation. For this test, the tablets have been formed by varying tablet mass, these are 100 mg and 200 mg tablets and by varying compaction strength, these are 0.75, 1 and 1.25 Metric Ton.

For the measurement of tablet strength, the tablets are placed on a spring-loaded manual compaction device. The tablets are placed vertically, and the compressive force is applied on the tablets and the strength is noted down in terms of kgf. Four tablets at each compaction strength of both 100 mg and 200 mg tablets have been measured. The stress generated inside the tablet has been calculated from the flowing relation (Fell and Newton, 1970):

$$\sigma = \frac{2F}{\pi D t} \qquad 4.6$$

4.4.1 Tablet strength of Avicel PH 101

This graph has been made when compression force of 0.75 Metric Ton is applied to the tablet.

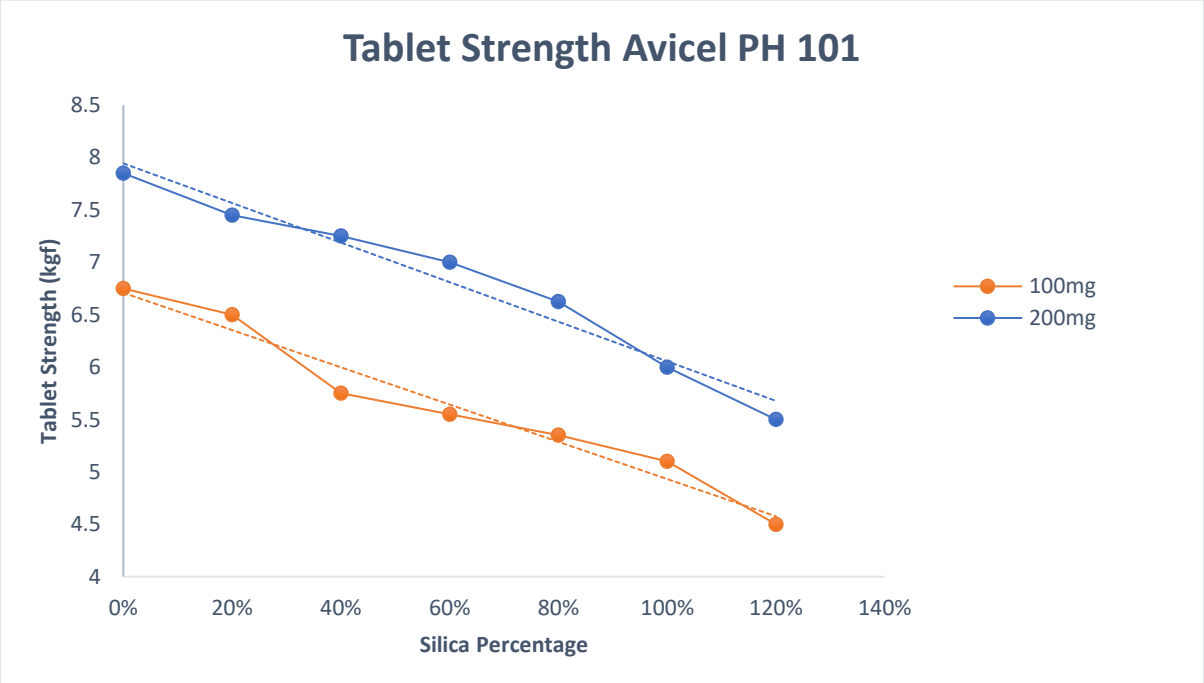

Fig 4.15: Tablet strength of Avicel PH 101 by varying tablet size and SAC

The observations made regarding the experiment are as follows:

With increase in the mass of the tablet, the tablet strength increases. This can be attributed to the increase in tablet dimensions (the tablet thickness) (Fell and Newton, 1970) through which the average force applied on the tablet increases.

Table 4.11: Tablet strength of Avicel PH 101 by varying tablet size

Product	100 mg Tablets Force (kPa)	200 mg Tablets Force (kPa)	Percentage increase in strength
Avicel PH 101	6.75	7.85	16.29
20% SAC	6.5	7.45	14.61
40% SAC	5.75	7.25	26.08
60% SAC	5.55	7	26.12
80% SAC	5.35	6.625	23.31
100% SAC	5.1	6	17.64
120% SAC	4.5	5.5	22.22

There is an average increase of ~20.89% tablet strength for 200 mg tablets over 100 mg tablets.

4.4.2 Tablet strength of Avicel PH 102

Similar to the above experimentation, the strength of Avicel PH 102 tablets is calculated at 0.75 Metric Ton.

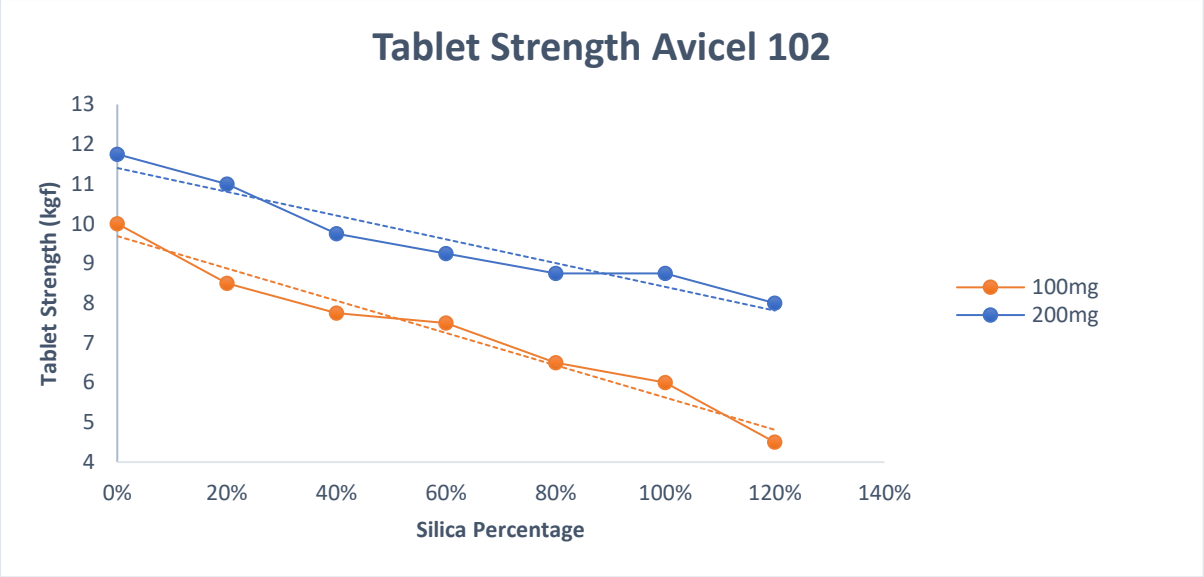

Fig 4.16: Tablet strength of Avicel PH 102 by varying tablet size and SAC

The observations made regarding the experiment are as follows:

With increase in the mass of the tablet, the tablet strength increases. This can be attributed to the increase in tablet dimensions (the tablet thickness) (Fell and Newton, 1970) through which the average force applied on the tablet increases.

Table 4.12: Tablet strength of Avicel PH 102 by varying tablet size

Product	100 mg Tablets Force (kPa)	200 mg Tablets Force (kPa)	Percentage increase in strength
Avicel PH 102	10	11.75	17.5
20% SAC	8.5	11	37.5
40% SAC	7.75	9.75	25.8
60% SAC	7.5	9.25	23.33
80% SAC	6.5	8.75	34.61
100% SAC	6	8.65	44.16
120% SAC	4.5	8.5	77.77

There is an average increase of ~37.23% tablet strength for 200 mg tablets over 100 mg tablets.

The validation for these results can be obtained from Narayan and Hancock (2005) where tablets have been compressed above 50 MPa (yield strength) and the tablet strength has been measured which validates the strength of "as received" Avicel PH 101 and Avicel PH 102.

4.4.3 Tablet strength of Avicel PH 101 with 100 mg tablet

These results have been measured for 100 mg tablets, by varying the compact force applied on the tablets. The tablets have been compacted at 0.75 Metric Ton, 1 Metric Ton and 1.25 Metric Ton. The results are as follows:

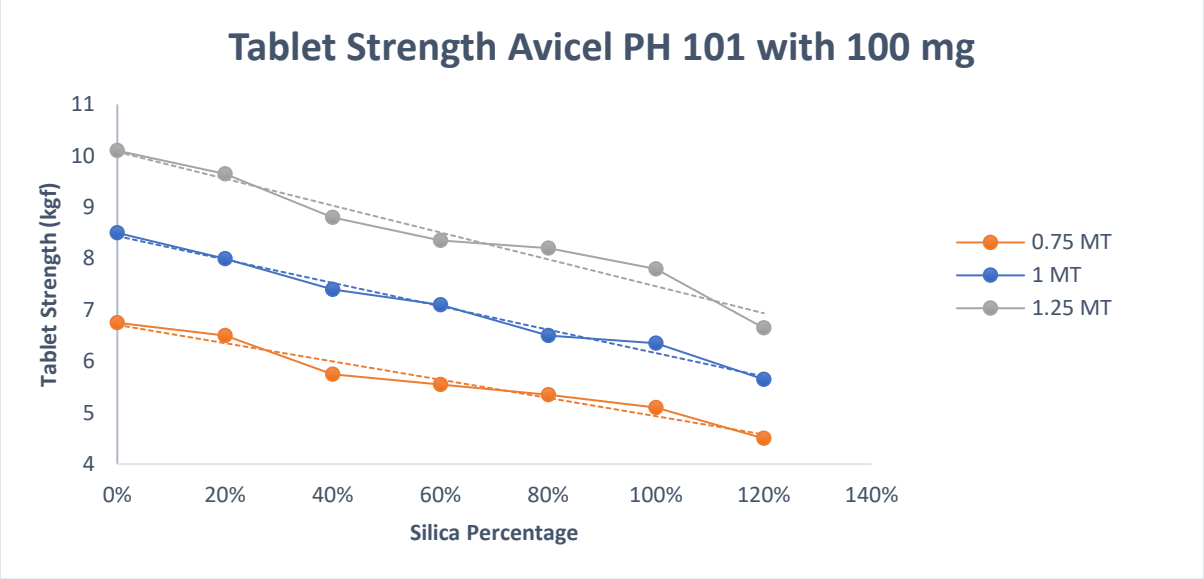

Fig 4.17: Tablet strength of 100 mg Avicel PH 101 varying compacting force and SAC

The observations that have been made regarding the experiment are as follows:

The increase in compaction force attributes to the increase in tablet strength.

Table 4.13: Tablet strength of 100 mg Avicel PH 101 varying compacting strength

Product	0.75 Metric Ton Tablet	1 Metric Ton Tablet		1.25 Metric Ton Tablet	
	Force (kgf)	Force (kgf)	w.r.t. 0.75 Metric Ton tablets	Force (kgf)	w.r.t. 0.75 Metric Ton tablets
Avicel PH 101	6.75	8.5	1.25	10.1	1.49
20% SAC	6.5	8	1.23	9.65	1.48

40% SAC	5.75	7.4	1.28	8.8	1.53
60% SAC	5.55	7.1	1.27	8.35	1.5
80% SAC	5.35	6.5	1.21	8.2	1.53
100% SAC	5.1	6.35	1.24	7.8	1.52
120% SAC	4.5	5.65	1.25	6.65	1.47

The average increase in tablet strength compared to 0.75 Metric Ton tablets, when compactive force is 1 Metric Ton is ~1.24 times. The average tablet strength when compactive force is 1.25 Metric Ton is ~1.502 times as compared to 0.75 Metric Ton tablets.

4.4.4 Tablet strength of Avicel PH 101 with 200 mg tablet

These results have been measured for 200 mg tablets by varying the compaction force applied on the tablets. The tablets have been compacted at 0.75, 1 and 1.25 Metric Ton. The results are as follows:

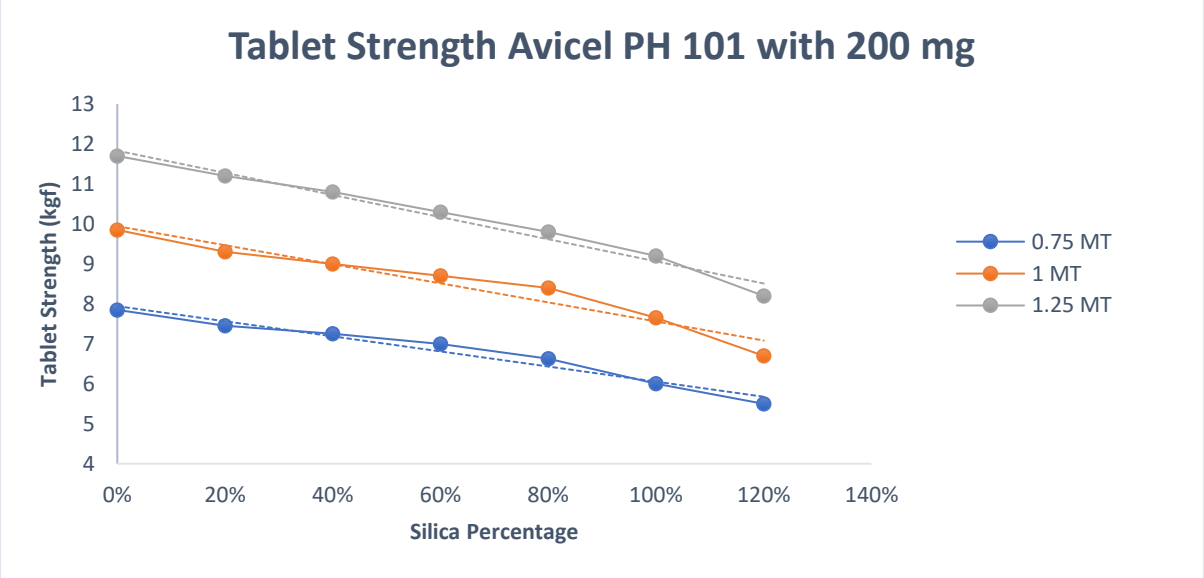

Fig 4.18: Tablet strength of 200 mg Avicel PH 101 varying compacting force and SAC

The observations that have been made regarding the experiment are as follows:

The increase in compaction force attributes to the increase in tablet strength.

Table 4.14: Tablet strength of 200 mg Avicel PH 101 varying compacting force

Product	0.75 Metric Ton Tablet	1 Metric Ton Tablet		1.25 Metric Ton Tablet	
	Force (kgf)	Force (kgf)	w.r.t. 0.75 Metric Ton tablets	Force (kgf)	w.r.t. 0.75 Metric Ton tablets
Avicel PH 101	7.85	9.85	1.25	11.7	1.49
20% SAC	7.45	9.3	1.24	11.2	1.5
40% SAC	7.25	9	1.24	10.8	1.48
60% SAC	7	8.7	1.24	10.3	1.47
80% SAC	6.625	8.4	1.26	9.8	1.47
100% SAC	6	7.65	1.27	9.2	1.53
120% SAC	5.5	6.7	1.21	8.2	1.49

The average increase in tablet strength compared to 0.75 Metric Ton tablets, when compactive force is 1 Metric Ton is ~1.244 times. The average tablet strength when compactive force is 1.25 Metric Ton is ~1.49 times as compared to 0.75 Metric Ton tablets.

4.4.5 Tablet strength of Avicel PH 102 with 100 mg tablet

These results have been measured for 100 mg tablets by varying the compact force applied on the tablets. The tablets have been compacted at 0.75, 1 and 1.25 Metric Ton. The results are as follows:

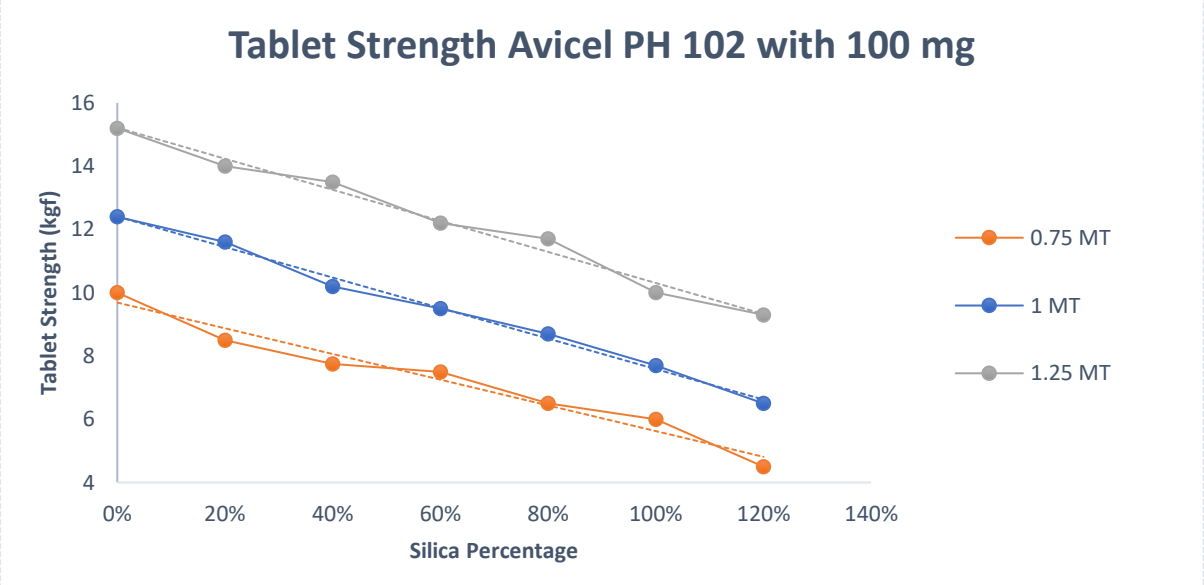

Fig 4.19: Tablet strength of 100 mg Avicel PH 102 varying compacting force and SAC

The observations that have been made regarding the experiment are as follows:

The increase in compaction force attributes to the increase in tablet strength.

Table 4.15: Tablet strength of 100 mg Avicel PH 102 varying compacting force

Product	0.75 Metric Ton Tablet	1 Metric Ton Tablet		1.25 Metric Ton Tablet	
	Force (kgf)	Force (kgf)	w.r.t. 0.75 Metric Ton tablets	Force (kgf)	w.r.t. 0.75 Metric Ton tablets
Avicel PH 102	10	12.4	1.24	15.2	1.52
20% SAC	8.5	11.6	1.36	14	1.64
40% SAC	7.75	10.2	1.31	13.5	1.61
60% SAC	7.5	9.5	1.26	12.2	1.62
80% SAC	6.5	8.7	1.33	11.7	1.8
100% SAC	6	7.7	1.28	10	1.66
120% SAC	4.5	6.5	1.44	9.3	2.06

The average increase in tablet strength compared to 0.75 Metric Ton tablets, when compactive force is 1 Metric Ton is ~1.318 times. The average tablet strength when compactive force is 1.25 Metric Ton is ~1.701 times as compared to 0.75 Metric Ton tablets.

4.4.6 Tablet strength of Avicel PH 102 with 200 mg tablet

These results have been measured for 200 mg tablets by varying the compact force applied on the tablets. The tablets have been compacted at 0.75, 1 and 1.25 Metric Ton. The results are as follows:

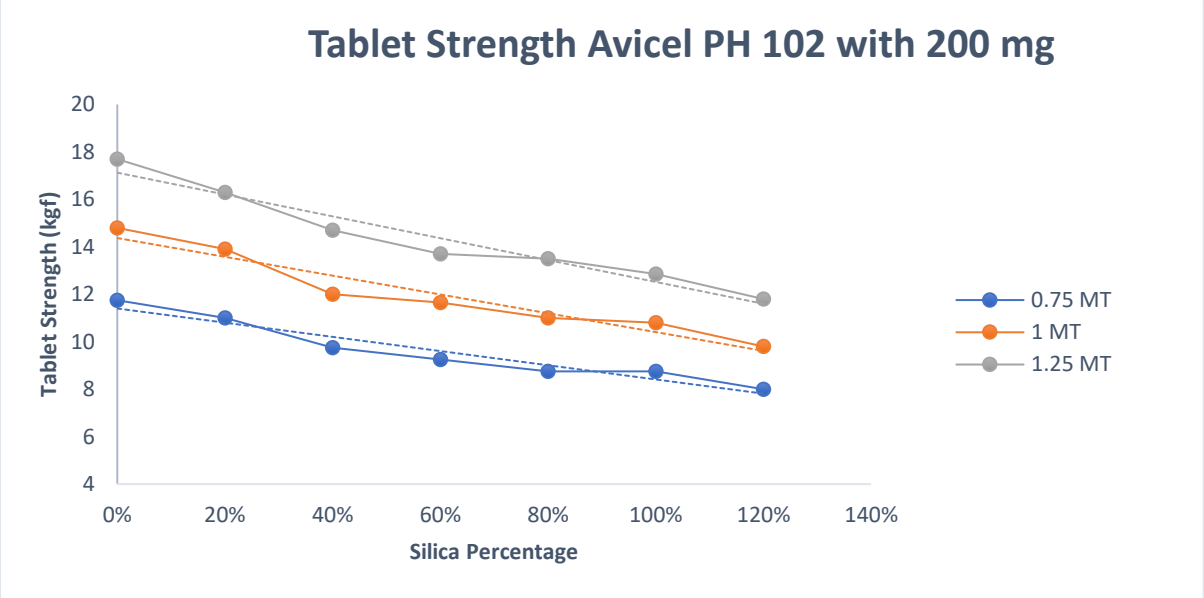

Fig 4.20: Tablet strength of 200 mg Avicel PH 102 varying compacting force and SAC

The observations that have been made regarding the experiment are as follows:

The increase in compaction force attributes to the increase in tablet strength.

Table 4.16: Tablet strength of 200 mg Avicel PH 102 varying compacting force

Product	0.75 Metric Ton Tablet	1 Metric Ton Tablet		1.25 Metric Ton Tablet	
	Force (kgf)	Force (kgf)	w.r.t. 0.75 Metric Ton tablets	Force (kgf)	w.r.t. 0.75 Metric Ton tablets
Avicel PH 102	11.75	14.8	1.25	17.7	1.506
20% SAC	11	13.9	1.26	16.3	1.48
40% SAC	9.75	12	1.23	14.7	1.507
60% SAC	9.25	11.65	1.259	13.7	1.48
80% SAC	8.75	11	1.257	13.5	1.54
100% SAC	8.65	10.8	1.248	12.85	1.48
120% SAC	8.5	9.8	1.15	11.8	1.388

The average increase in tablet strength compared to 0.75 Metric Ton tablets, when compactive force is 1 Metric Ton is ~1.236 times. The average tablet strength when compactive force is 1.25 Metric Ton is ~1.483 times as compared to 0.75 Metric Ton tablets.

Comparing all the different combinations of compaction forces, the tablets associated with it, the biggest rise in the tablet strength are 100 mg Avicel PH 102 with 120% SAC samples. The maximum force required to break the tablets that has been observed is 17.7 kgf in “as received” Avicel PH 102 particles having the tablet weight of 200 mg.

Chapter 5

Conclusion and Future Scope

Conclusion

From the above results, it can be safely concluded that there is an improvement in the flowability of the powders after the addition of glidant. Earlier, both the powders were in the easy flowing region, during the "as received" flow function test and Avicel PH 102 had better flowability as compared to Avicel PH 101. But with the addition to R972 silica, Avicel PH 101 showed more change than Avicel PH 102, so much so that after the addition, 5 out of 7 combinations of silica R972 and Avicel PH 101 showed flowability in the free-flowing region, but there is a negligible increase in flowability between 80-120% SAC samples of Avicel PH 101. Whereas, in the case of Avicel PH 102 only 120% SAC case showed the flowability in the free-flowing region. This implies that Avicel PH 102 has less affinity to change with addition of R972 silica.

Wall friction angle is another important parameter measured and the results from the testing show that wall friction definitely increases with increase in R972 silica, but there is no specific trend on how this parameter will change on a practical use. Further, this parameter is used for the calculation of hopper half angle which uses both flow function test values in addition to wall friction test values. The trend in the change in hopper half angle with addition of R972 silica shows, at a certain hopper opening diameter, the powder with higher silica content is able to flow at a higher hopper half angles as compared to as received Micro-crystalline cellulose powders.

Another important parameter calculated which is useful from the mass production point of view is tabletability. In this, at a certain compacting force, the force required to break the tablet increases as the mass of the tablet formed increases. The average increase in the tablet strength with increase in tablet mass from 100 mg to 200 mg for Avicel PH 101 is ~20.89% and for Avicel PH 102 is ~37.23%. And with the increase in compaction force from 0.75 Metric Ton to 1 Metric Ton and 1.25 Metric Ton in Avicel PH 101 samples, there is an average linear increase of 25% tablet strength from 0.75 Metric Ton to 1 Metric Ton and 50% increase in tablet strength from 0.75 Metric Ton to 1.25 Metric Ton compaction. Whereas, higher increase in tablet strength has been observed when high compaction has been exerted on high silica

content powders. Up to 44% increase has been calculated when 120% SAC of silica is added in Avicel PH 102 in 100 mg tablets and 106% increase has also been calculated when 120% SAC of silica is added in Avicel PH 102 in 200 mg tablets.

So, if Avicel PH 101 has to be used then 80% SAC silica with 1 MT force on 200 mg tablet is recommended for good flowability and tablet formation. While, if Avicel PH 102 is to be selected for blend then 120% SAC silica with 1.25 MT force on 100 mg tablet is recommended.

Future Scope

An investigation of flowability and flow properties of the above powders with the help of various dry coating machines such as MAIC, V-Blender, Co-mill mixture with the help of Brookfield PFT.

The flow properties through hoppers and tabletability have been investigated. However, the maximum time for the powders are spent flowing the pipes where the powder flows as a two-phase flow system.

It is known that the powders with particle diameter belonging to geldart C group form channels in the flow from where air passes without having an effect over the powder itself. And the same powder has problems flowing through the hoppers as van der Waal forces of adhesion increases resulting in resistance to flow. But there is no direct correlation to the two flow problems.

References

Amagliani, L., O'Regan, J., Kelly, A.L. and O'Mahony, J.A., 2016. Chemistry, structure, functionality and applications of rice starch. *Journal of Cereal Science, 70*, pp.291-300.

Attia, U.M., Fones, A., Trepleton, R., Hamilton, H., Davies, S. and Wimpenny, D., 2014. HIPing of Pd-doped titanium components: A study of mechanical and corrosion properties. *The 11th International Conference of Hot Isostatic Pressing (HIP '14)*

A. V. Shenoy, D. R. Saini., 1986. Melt Flow Index, More than Just a Quality Control Parameter. Part I., *Advances in Polymer Technology*, Vol. 6, No. 1, pages 1–58.

Bian, Q., Sittipod, S., Garg, A. and Ambrose, R.K., 2015. Bulk flow properties of hard and soft wheat flours. *Journal of Cereal Science*, *63*, pp.88-94.

Chen, L., Ding, X., He, Z., Huang, Z., Kunnath, K.T., Zheng, K. and Davé, R.N., 2018. Surface engineered excipients: I. improved functional properties of fine grade microcrystalline cellulose. *International Journal of Pharmaceutics*, *536*(1), pp.127-137.

Chen, L., Ding, X., He, Z., Fan, S., Kunnath, K.T., Zheng, K. and Davé, R.N., 2018. Surface engineered excipients: II. Simultaneous milling and dry coating for preparation of fine-grade microcrystalline cellulose with enhanced properties. *International Journal of Pharmaceutics*, *546*(1-2), pp.125-136.

Dudhat, S.M., Kettler, C.N. and Dave, R.H., 2017. To Study Capping or Lamination Tendency of Tablets Through Evaluation of Powder Rheological Properties and Tablet Mechanical Properties of Directly Compressible Blends. *AAPS PharmSciTech*, *18*(4), pp.1177-1189.

Faqih, A.M.N., Mehrotra, A., Hammond, S.V. and Muzzio, F.J., 2007. Effect of moisture and magnesium stearate concentration on flow properties of cohesive granular materials. *International Journal of Pharmaceutics*, *336*(2), pp.338-345.

Faqih, A.N., Alexander, A.W., Muzzio, F.J. and Tomassone, M.S., 2007. A method for predicting hopper flow characteristics of pharmaceutical powders. *Chemical Engineering Science*, *62*(5), pp.1536-1542.

Fell, J.T. and Newton, J.M., 1970. Determination of tablet strength by the diametral-compression test. *Journal of Pharmaceutical Sciences*, *59*(5), pp.688-691.

Fitzpatrick, J.J., Iqbal, T., Delaney, C., Twomey, T. and Keogh, M.K., 2004. Effect of powder properties and storage conditions on the flowability of milk powders with different fat contents. *Journal of Food Engineering*, *64*(4), pp.435-444.

Ganesan, V., Rosentrater, K.A. and Muthukumarappan, K., 2008. Flowability and handling characteristics of bulk solids and powders–a review with implications for DDGS. B*iosystems Engineering*, *101*(4), pp.425-435.

Garg, V. and Mallick, S.S., 2017. An Experimental Investigation into the Flow Properties of Pharmaceutical and Detergent Powders (Master's dissertation).

Grey, R.O. and Beddow, J.K., 1969. On the Hausner ratio and its relationship to some properties of metal powders. *Powder Technology*, *2*(6), pp.323-326.

Geldart, D., 1972. The effect of particle size and size distribution on the behaviour of gas-fluidised beds. *Powder Technology*, *6*(4), pp.201-215.

Geldart, D., 1973. Types of gas fluidization. *Powder Technology*, *7*(5), pp.285-292.

Geldart, D., Harnby, N. and Wong, A.C., 1984. Fluidization of cohesive powders. *Powder Technology*, *37*(1), pp.25-37.

Geldart, D., Abdullah, E.C., Hassanpour, A., Nwoke, L.C. and Wouters, I., 2006. Characterization of powder flowability using measurement of angle of repose. *China Particuology*, *4*(03n04), pp.104-107.

Gabaude, C.M.D., Gautier, J.C., Saudemon, P. and Chulia, D., 2001. Validation of a new pertinent packing coefficient to estimate flow properties of pharmaceutical powders at a very early development stage, by comparison with mercury intrusion and classical flowability methods. *Journal of Materials Science*, *36*(7), pp.1763-1773.

Guo, A., Beddow, J.K. and Vetter, A.F., 1985. A simple relationship between particle shape effects and density, flow rate and Hausner ratio. *Powder Technology*, *43*(3), pp.279-284.

Iqbal, T. and Fitzpatrick, J.J., 2006. Effect of storage conditions on the wall friction characteristics of three food powders. *Journal of Food Engineering*, *72*(3), pp.273-280.

Jenike, A.W., 1961. Gravity Flow of Bulk Solids. University of Utah Engineering Experiment Station. *Bulletin*, *108*.

Jenike, A.W., 1964. Storage and Flow of Solids. University of Utah Engineering Experiment Station. *Bulletin*, *123*.

Jenike, A.W., 1987. A theory of flow of particulate solids in converging and diverging channels based on a conical yield function. *Powder Technology*, *50*(3), pp.229-236.

Ji, J., Fitzpatrick, J., Cronin, K., Fenelon, M.A. and Miao, S., 2017. The effects of fluidised bed and high shear mixer granulation processes on water adsorption and flow properties of milk protein isolate powder. *Journal of Food Engineering*, *192*, pp.19-27.

Koynov, S., Glasser, B. and Muzzio, F., 2015. Comparison of three rotational shear cell testers: Powder flowability and bulk density. *Powder Technology*, *283*, pp.103-112.

Li, R., Roos, Y.H. and Miao, S., 2016. The effect of water plasticization and lactose content on flow properties of dairy model solids. *Journal of Food Engineering*, *170*, pp.50-57.

Lumay, G., Boschini, F., Traina, K., Bontempi, S., Remy, J.C., Cloots, R. and Vandewalle, N., 2012. Measuring the flowing properties of powders and grains. *Powder Technology*, *224*, pp.19-27.

Macrì, D., Barletta, D., Lettieri, P. and Poletto, M., 2017. Experimental and theoretical analysis of TiO_2 powders flow properties at ambient and high temperatures. *Chemical Engineering Science*, *167*, pp.172-190.

Massimilla, L. and Donsì, G., 1976. Cohesive forces between particles of fluid-bed catalysts. *Powder Technology*, *15*(2), pp.253-260.

Michrafy, A., Kadiri, M.S. and Dodds, J.A., 2003. Wall friction and its effects on the density distribution in the compaction of pharmaceutical excipients. *Chemical Engineering Research and Design*, *81*(8), pp.946-952.

Morin, G. and Briens, L., 2013. The effect of lubricants on powder flowability for pharmaceutical application. *Aaps Pharmscitech*, *14*(3), pp.1158-1168.

Morin, G. and Briens, L., 2014. A comparison of granules produced by high-shear and fluidized-bed granulation methods. *AAPS PharmSciTech*, *15*(4), pp.1039-1048.

Narayan, P. and Hancock, B.C., 2005. The influence of particle size on the surface roughness of pharmaceutical excipient compacts. *Materials Science and Engineering: A*, *407*(1-2), pp.226-233.

Ripp, M., Debele, Z.A. and Ripperger, S., 2015. Determination of Bulk Flow Property of tef Flour and Seed and Design of a Silo. *Particulate Science and Technology*, *33*(5), pp.494-502.

Rohilla, L., Mallick, S.S. and Setia, G., 2016. An Experimental Investigation on the Flow Properties of Bulk Solids (Master's dissertation).

Schulze, D., 2008. Powders and bulk solids. Behaviour, Characterization, Storage and Flow. *Springer*.

Sun, C.C., 2016. Quantifying effects of moisture content on flow properties of microcrystalline cellulose using a ring shear tester. *Powder Technology*, *289*, pp.104-108.

Sun, C.C. and Himmelspach, M.W., 2006. Reduced tabletability of roller compacted granules as a result of granule size enlargement. *Journal of Pharmaceutical Sciences*, *95*(1), pp.200-206.

Trementozzi, A.N., Leung, C.Y., Osei-Yeboah, F., Irdam, E., Lin, Y., MacPhee, J.M., Boulas, P., Karki, S.B. and Zawaneh, P.N., 2017. Engineered particles demonstrate improved flow properties at elevated drug loadings for direct compression manufacturing. *International Journal of Pharmaceutics*, *523*(1), pp.133-141.

Wang, Y., Koynov, S., Glasser, B.J. and Muzzio, F.J., 2016. A method to analyze shear cell data of powders measured under different initial consolidation stresses. *Powder Technology*, *294*, pp.105-112.

Wouters, I.M. and Geldart, D., 1996. Characterising Semi-Cohesive Powders using angle of repose. *Particle and Particle Systems Characterization*, *13*(4), pp.254-259.

Yang, W.C., 2007. Modification and re-interpretation of Geldart's classification of powders. *Powder Technology*, *171*(2), pp.69-74.

Yang, J., Sliva, A., Banerjee, A., Dave, R.N. and Pfeffer, R., 2005. Dry particle coating for improving the flowability of cohesive powders. *Powder Technology*, *158*(1-3), pp.21-33